

1

The Influence of Fluvial and Glacial Watershed Dynamics on Holocene Sediment Accumulation in Cariboo Lake, Columbia Mountains, British Columbia, Canada

Journal Title

XX(X):2–45

©The Author(s) 0000

Reprints and permission:

sagepub.co.uk/journalsPermissions.nav

DOI: 10.1177/ToBeAssigned

www.sagepub.com/

SAGE

² A. Cebulski^{*1,2}, J. Desloges²

Abstract

An acoustic record of sedimentation and sediment cores from Cariboo Lake are analyzed to present a high-resolution record of sediment accumulation. Acoustically penetrable sediment reaches a maximum thickness of 35 m in deep parts of the lake, representing deglacial and Holocene accumulation. A transition from massive to well-layered sediments is observed in the sub-bottom acoustic record during final phases of valley deglaciation in the region (ca. 10.5-9 ka BP). Fine clastic sediments produced from the glaciated headwaters are delivered by Cariboo River as over-flow currents into the lake which produce bimodal rhythmic layering of silt and clay sediments. Laminae couplets are inferred to be

³ deposited annually according to two AMS radiocarbon dates and a varve counting chronology. Two long cores, 2.9 and 3.8 m in length, were selected for analysis with estimated basal dates of 2 ka BP. The accumulation of sediment into Cariboo Lake shows above average sediment accumulation rates between 0-700CE and 1500-2017CE which are coincident with cool temperatures and peak glacier extents. Cariboo Lake is situated in the northern Columbia Mountains, British Columbia, Canada and is representative of environments transitioning from semi-arid interior climates to glaciated high mountain regions to the east. The sediment chronology presented in this study contributes to the existing body of knowledge of lake sediment accumulation and Holocene watershed activity for this transitional climate region of western Canada.

Keywords

⁴ Glaciolacustrine; Sediment; Holocene; Connectivity; Varve; British Columbia

Introduction

⁵ Environmental proxies that extend back beyond the modern observable record are crucial
⁶ to understanding earth system processes (Turney et al., 2019; Huber and Knutti, 2012;
⁷ Nelson et al., 2016). Proxy reconstructions at the sub-annual scale (e.g. ice cores,

¹Centre for Hydrology, University of Saskatchewan, Canmore, Canada

²Department of Geography and Department of Earth Sciences, University of Toronto, Toronto, Canada

Corresponding author:

Alex Cebulski

Email: alexcebulska@gmail.com

tree rings, and corals), to multi-decadal scales (e.g. sediments, pollen, boreholes) have proven useful in describing past environmental conditions across the globe (Masson-Delmotte et al., 2013). In the case of sedimentary sequences collected from climate sensitive glaciated watersheds, they have been important in contributing to the regional understanding of climate and hydrologic variability over the Holocene. For example, research by Neukom et al. (2019) have utilized sedimentary sequences as part of larger paleolimnological collections to provide global reconstructions of temperature variability over the last 2000 years.

Climatic variability in western Canada over the Holocene contributed to several fluctuations in glacial activity with implications for sediment accumulation in glacier-fed lakes. Multi-proxy analyses of lake sediments from Vancouver Island (Brown et al., 2006), south central British Columbia (Lowe et al., 1997) and northern Washington State (Steinman et al., 2019) suggest low lake levels and precipitation amounts during the early Holocene around 11.0 to 7.50 ka. Reduced glacier extents in western Canada are found during the early Holocene in the southern Coast Mountains (Menounos et al., 2004; Koch et al., 2007; Osborn et al., 2007) and Canadian Rocky Mountains (Luckman, 1988, 1993) have been found to be reduced relative to the late Holocene. During the Early Neoglacial (7.50-5.00 ka), glaciers increased in extent in the south Coast Mountains (Osborn et al., 2007; Filippelli et al., 2006; Ryder and Thomson, 1986; Harvey et al., 2012) with some limited evidence in the Interior ranges and Rocky Mountains (Luckman, 1993). During the Early-middle Neoglacial (5.00-3.50 ka), there is widespread evidence of at least two glacial advances across western Canada from material dated in glacial forefields and glacier-fed lakes (Koch et al., 2007; Osborn et al., 2007; Menounos and Clague, 2008; Gardner and Jones, 1985; Wood and Smith, 2004; Hodder et al., 2006; Desloges, 1999; Leonard and Reasoner, 1999). During the Middle-late Neoglacial (3.50-1.00 ka), two periods of glacier advance have been reported. In the central and eastern ranges of Canada, records support extensive glacier coverage around 3.5-2.77 ka and 1.8-1.5 ka from lacustrine sediment records (Leonard and Reasoner, 1999; Leonard, 1997; Dirsztowsky and Desloges, 1997; Desloges, 1999) and from log and stump material between (Wood and Smith, 2004; Luckman, 1995; Luckman et al., 1999). The Little Ice Age (LIA) includes glacier advances over the past millennium and have been reported as broadly synchronous from Alaska to Patagonia (Luckman, 2000). In the Canadian Rocky Mountains many glaciers reached peak glacier extents during the LIA, and are estimated to be centered

44 around 1250 CE (Luckman, 1995; Osborn et al., 2001; Leonard, 1997) and 1850 CE
45 (Luckman and Kavanagh, 2000; Leonard, 1997). Over the Holocene there is general
46 regional agreement on the timing and magnitude of the large Early Holocene retreat
47 and Late Holocene LIA advance however, the smaller fluctuations that occurred
48 between these large events have less regional agreement (Menounos et al., 2009).

49 In the western Cordillera of Canada, sedimentary sequences have been collected
50 to better understand the hydroclimatic and glacial history of the Coast Mountains
51 (Menounos and Clague, 2008), St. Elias Mountains (Crookshanks and Gilbert, 2008),
52 Monashee Mountains (Hodder et al., 2006), and Rocky Mountains (Leonard, 1986;
53 Dirsztowsky and Desloges, 1997; Desloges, 1999). A study by Gilbert and Desloges
54 (2012) of Quesnel Lake (272 km²), 30 km south of the study area examined here, found
55 deglacial, and the very earliest Holocene, sediment infills to be high at around 10.4
56 ka BP, declining significantly at around 8.4 ka BP. Trends in Quesnel Lake sediment
57 characteristics during the Holocene were not detectable as accumulation rates were very
58 low in the areas of the lake that could be sampled. Quesnel Lake is very large relative to
59 the contributing watershed and therefore the sediment system is much less sensitive to
60 climate variability. Within the Cariboo Lake basin, Maurer et al. (2012) investigated
61 On-off Lake which remained intermittently connected to the Castle Creek Glacier
62 on the basin divide (Figure 1). Currently the Castle Creek Glacier resides outside
63 of the Cariboo Lake basin, however Maurer et al. (2012) provide evidence that
64 the glacier advanced across the hydrological divide and into the Cariboo Lake
65 basin several times over the Holocene. Advances of the Castle Creek Glacier into
66 the Cariboo Lake basin occurred around around 4.96-4.45, 2.73-2.49, 1.87-1.72,
67 and 1.54-1.42 ka BP (Maurer et al. (2012)). Both Gilbert and Desloges (2012) and
68 Maurer et al. (2012) provide a long but coarse resolution record of the fluvial and
69 glacial activity of the Cariboo Mountains. Additional high resolution records for this
70 transitional climate between the wetter Coastal and drier Rocky Mountain ranges
71 are needed especially for the mid to late Holocene interval where greater regional
72 variability in glacial responses to climate change has been observed (Steinman et al.,
73 2019; Menounos et al., 2009).

74 Previous studies on glacier-fed lakes have had success relating lake bottom
75 sediment archives (e.g. varves thickness, grain size and organic content) to
76 changes in regional temperature, precipitation patterns, and glacier extent over the
77 Holocene (Desloges, 1999; Hodder et al., 2006; Leonard, 1997; Menounos et al.,

78 **2006; Menounos and Clague, 2008).** Mountain basins that exhibit a strong nival-
79 hydrographic regime typically produce distinct varve couplets with a fine-grained
80 layer deposited in winter when the lake ices over and flow velocity decreases
81 followed by a coarse-grained layer deposited during spring high flows (e.g. Leonard,
82 1997; Hodder et al., 2007; Desloges, 1999). In contrast, lakes proximal to the Coast
83 Mountains of British Columbia typically show greater variability in varve thickness
84 due to the influence of frequent and large fall rain storms that produce multiple
85 coarse laminations within a single season (e.g. Gilbert et al., 1997; Menounos and
86 Clague, 2008).

87 Lakes that are more distal from glacier sources typically have relatively lower
88 sediment inputs and finer grain sizes, due to the upstream filtering of river
89 floodplains and lakes (Hodder et al., 2007). The effect of this filtering can influence
90 the climate and hydrology signals and may contribute to a weaker signal to noise
91 ratio and reduced sensitivity to hydroclimatic variability (Jerolmack and Paola,
92 2010).

93 Establishing a correlation between seasonal or annual trends in varve thickness,
94 grain size, and organic content from sediment cores to local discharge, temperature,
95 and precipitation is not always possible due to complex process interactions (Hodder
96 et al., 2007; Menounos and Clague, 2008; Heideman et al., 2018). The linkage
97 between the lake sediment record with hydrology and climate drivers is typically
98 weak at time scales less than 10 years (Hodder et al., 2007; Menounos and Clague,
99 2008; Heideman et al., 2018). Trends in lake sediment sequences are typically more
100 representative of climate fluctuations at longer time scales greater than 100 years
101 (Leonard and Reasoner, 1999; Osborn et al., 2007; Heideman et al., 2018).

102 Sediment chronologies in clastic lake sediments are typically derived from a
103 combination of radiocarbon dating (Gilbert and Desloges, 2012; Hodder et al., 2006;
104 Steinman et al., 2019), identification of volcanic tephra layers (Gilbert and Desloges,
105 2012; Hodder et al., 2006; Steinman et al., 2019) and counting of visible annual
106 laminations (varves) (Hodder et al., 2006; Heideman et al., 2015). The Mt. Mazama
107 volcanic eruption is the most prominent tephra layer typically found in sediment
108 sequences in western Canada (Gilbert and Desloges, 2012; Steinman et al., 2019)
109 and has been dated to approximately 7600 cal. BP (Zdanowicz et al., 1999; Hallett
110 et al., 1997). Westgate (1977) reports the most recent major volcanic ash event to
111 reach central BC occurred 2100 yr BP, predating the basal age of the four sediment
112 cores presented in this study.

113 Few sedimentary sequences exist in central British Columbia that provide a
114 high resolution and long term record of hydroclimatic variability (**Gilbert and**
115 **Desloges, 2012; Hodder et al., 2006; Menounos et al., 2009; Maurer et al., 2012**). The
116 sedimentary sequence from Cariboo Lake presented here, fills this gap by providing
117 a new record of Holocene hydroclimatic variability for the transitional zone between
118 the Coastal and Rocky Mountains from lake bottom sediment records recovered
119 using sub-bottom acoustic methods and long sediments cores.

120 The purpose of this research is to 1) establish an understanding of the mechanisms that
121 control the delivery and deposition of the fine sediment fraction to Cariboo Lake, 2) to
122 reconstruct the highest resolution and longest possible sediment accumulation record
123 from cores and acoustic methods for this area of British Columbia, 3) compare and
124 contrast the accumulation record in this transitional (semi-arid to glaciated mountainous)
125 lake system with existing sedimentary sequences and regional climate proxies in western
126 Canada.

127 Study Area

128 Cariboo Lake is located in the northern foothills of the Columbia Mountains, 85 km
129 northeast of Williams Lake, British Columbia (Figure 1). The lake receives runoff from
130 an area of 3244 km², which is filtered by three deep fjord like lakes: Issac Lake, Lanezi
131 Lake, and Ghost Lake shown in Figure 1. The watershed relief ranges from 2600 m
132 asl. in the eastern headwaters to 600 m asl. at the western Cariboo Lake outlet. The
133 west to east, 90 km long watershed spans a precipitation gradient ranging from 1370
134 mm yr⁻¹ in the headwaters to 477 mm yr⁻¹ at the semi-arid outlet to the lake. The area
135 of Cariboo Lake is 10 km² resulting in a lake area-to-watershed area ratio of 0.3%.
136 The Cariboo Lake watershed has 64 km² of permanent ice cover which covers 2% of
137 the total watershed (**Bolch and Bolch, 2008**). The most extensive glaciated terrain is
138 proximal to Mt. Lunn roughly 60 km upstream of Cariboo Lake (Figure 1). **The Cariboo**
139 **Lake basin hydrology is snow- and glacier-melt dominant with average 1971-2000**
140 **monthly runoff peaking in June and low-flows that occur between December and**
141 **March (Figure 2, A). From December to March the air temperature is mostly below**
142 **0 °C and precipitation falls primarily as snow during these months (Figure 2).**

143 The Cariboo River, draining into the east margin of the lake, is the main source of
144 sediment. The lake is separated into two basins by a large alluvial fan building cross-
145 valley from Keithley Creek (Figure 3). **The surface area of the upstream basin is**

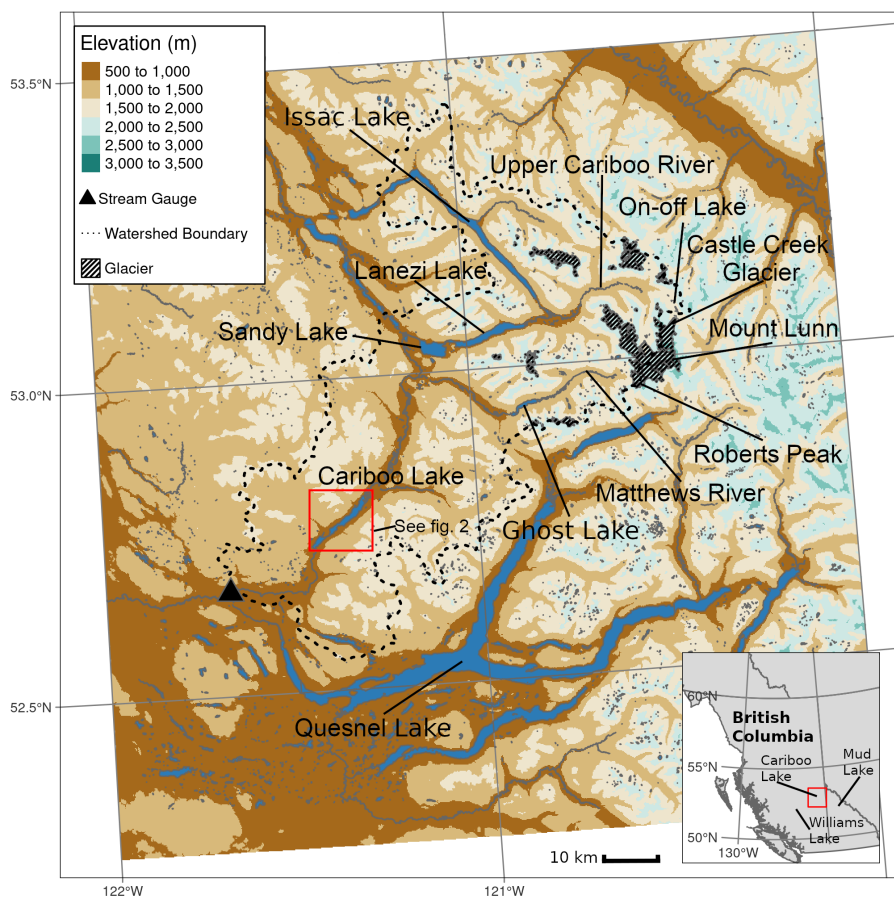


Figure 1. Map of the Cariboo Lake basin. Inset map shows the location of the Cariboo Lake basin within British Columbia relative to the Mud Lake basin from the Hodder et. al. (2006) study. See Figure 2 for detailed map of Cariboo Lake.

146 **8 km²** and is referred to here as the main Cariboo Lake basin. The downstream
 147 basin, referred to here as the Keithley Creek sub-basin, is 2 km² in surface area.
 148 The bathymetry of the lake reaches a maximum depth of over 50 m in two deep
 149 holes within the central part of the main Cariboo Lake basin. These deep holes
 150 provide some evidence of past glacial scouring and ice extents that reached the lake.

151 Lanezi Lake is a deep fjord-like lake with a flat lake bottom bathymetry reaching
 152 a maximum depth of 170 m and suggests sediment delivery to this lake has been

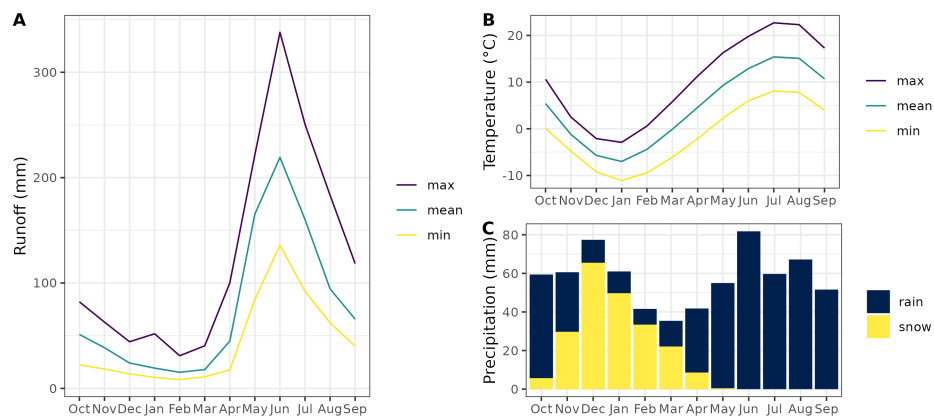


Figure 2. 1971-2000 monthly runoff statistics for Water Survey of Canada station 08KH003 (A) and 1971-2000 temperature and precipitation normals from Environment Canada station 1094616 (B). The top of each bar on panel C corresponds to the average monthly total precipitation and the coloured portion shows the fraction of rain or snow.

153 **relatively high over the Holocene (Figure 1).** Sandy Lake is much shallower reaching a
 154 maximum depth of 6 m. The Matthews River, which meets the Cariboo River just below
 155 Lanezi Lake provides a less filtered connection to meltwater sources draining several
 156 alpine glaciers including the largest area of ice (10 km^2) in the Cariboo Lake watershed,
 157 proximal to Roberts Peak (Figure 1).

158 Methods

159 Field Methods

160 A field campaign was conducted during the summer of 2017 to collect sub-bottom
 161 acoustic soundings, dredge samples, and sediment cores. Thirty-four km of sub-bottom
 162 acoustic soundings were collected across Cariboo Lake using a 10 kHz StrataBox 3510
 163 HD. An Ekman dredge was used to collect 20 samples from the lake bottom, each
 164 yielding $\sim 730 \text{ cm}^3$ of surficial sediment. The dredge samples were sub-sampled in the
 165 field using an 80 mm diameter PVC cylinder pushed into the block of sediment. This
 166 resulted in 20 short cores each containing about 450 cm^3 of sediment. **The Ekman**
 167 **dredge filled with variable depths of sediment and as a result the short cores ranged**
 168 **from 6 to 12 cm in length.** The remaining sediment not captured in the PVC cylinder
 169 was kept as a bulk sediment sample. Four long sediment cores (V1-V4) were collected
 170 using a Rossfelder submersible vibracorer with a 6 m long 70 mm diameter aluminum

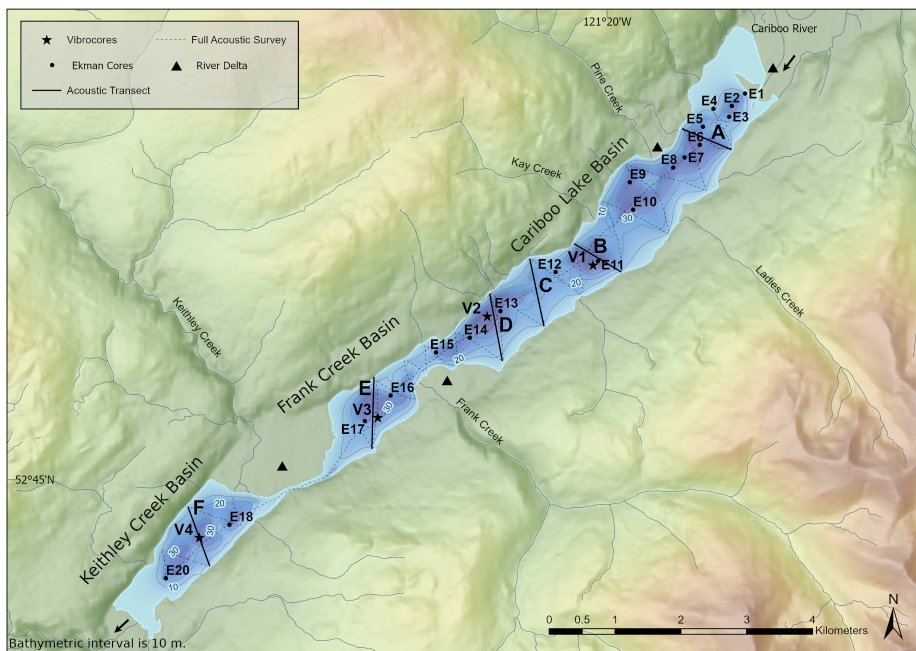


Figure 3. Map of the Cariboo Lake bathymetry and coring locations. Bathymetric interval is 10 m. Acoustic transects selected for analysis are shown with a black solid line and labeled A, B, C, D, E and F. Fan deltas mentioned in the text are represented by black triangles and are referenced to by the upstream creek (i.e. Frank Creek Delta is the triangle below Frank Creek). The Frank Creek fan delta separates the main Cariboo Lake and Frank Creek sub-basins. The Keithley Creek fan delta separates the Frank Creek and Keithley Creek sub-basins.

171 pipe. The Ekman short cores and the long vibracores were split longitudinally with one
 172 half preserved as an archive and the other as a working half. The working half samples
 173 were prepared for imaging by scraping the core parallel to the sediment laminae to create
 174 a flat surface which showed the sediment stratigraphy. **The stratigraphy of long cores**
 175 **V1 and V2 were selected for detailed analysis as they were located within the deepest**
 176 **parts of upper Cariboo Lake. The deep mid-lake sampling locations were important**
 177 **to ensure the cores consisted of a higher fraction of fine clastic sediments from**
 178 **the main Cariboo River compared to coarser sediments derived from steep valley**
 179 **sidewalls and turbidite flood events. Cores V3 and V4 taken at shallower depths**
 180 **further down-lake had higher fractions of coarse grained sediments and resulted in**

181 a higher degree of core disturbance, presumably due to the lower cohesion of the
182 coarser grained sediments.

183 *Laboratory Methods*

184 The cores and short cores were analyzed for laminae thickness, organic content, and
185 particle size. The working halves of long cores V1 and V2 were subsampled with 2
186 cm³ of sediment extracted at a 5 cm interval, with additional samples taken within
187 stratigraphic breaks. **Stratigraphic breaks were identified based on visual changes**
188 **in grain size and lamination patterns.** Laminae couplets observed on the **working**
189 **halves** were digitally counted and measured for thickness using the ImageJ software,
190 by Schneider et al. (2012). **Uncertainty in laminae counting is attributed to sections**
191 **of core with indiscernible laminae formation, core compaction, undercounting, and**
192 **subjectivity in classifying the occasionally thicker (4 to 47 mm thick) graded to**
193 **massive laminae/beds.** Varve counting uncertainties in the literature are reported
194 as ranging between 0.7 - 6 % (Menounos and Clague, 2008; Zolitschka, 1991).
195 The uncertainty of the laminae counting in this study was inferred from Ekman
196 short cores (E12, E13, E14) which had statistically similar sediment accumulation
197 rates. The varve counting error was estimated by counting the number of couplets
198 down to a specific depth of 5 cm in each Ekman core resulting in a standard
199 deviation between the counts for each core. The top section of cores V1 and V2
200 were disturbed during coring - 110 mm for V1 and 70 mm for V2 which prevented
201 counting and measurement of laminae couplets. Organic content was determined by
202 loss-on-ignition analysis (550 °C) following methods in Smith (2003). Samples were
203 first weighed to provide an initial wet weight, then dried at 60 °C and weighed again
204 after oven drying. The samples were then placed in a furnace at 550 °C for 2.5 hours
205 and weighed a third time. Grain size analysis was conducted using a Mastersizer Particle
206 Size Analyzer 3000. Samples were prepared following methods by Gray et al. (2010) to
207 remove the fine fraction of particles from organic material. This involved a removal of
208 organic material using three sequential aliquots of 20% H₂O₂ until the sample stopped
209 reacting. To prevent flocculation of sediment grains the samples were dispersed in 0.05%
210 solution of Calgon for 24 hours. Grain size was measured three times for each sample,
211 resulting in an average standard deviation of ± 0.01 µm. The chronology of both vibra
212 cores was reconstructed using AMS ¹⁴C dating (analyzed at the André E. Lalonde
213 AMS Laboratory at the University of Ottawa) and a chronology derived from laminae
214 (couplet) counting on working core images. The AMS ¹⁴C calibration was performed

215 using Bchron, a Bayesian statistical age-model software package for R (Parnell et al.,
216 2008, 2011; Haslett and Parnell, 2008) and the IntCal13 calibration curve (Reimer et al.,
217 2013).

218 **Results**

219 *Sub-bottom Acoustics*

220 Acoustic stratigraphy from six selected transects (see locations in Figure 3) reveal the
221 range of morphologies and character of sedimentary deposits in Cariboo Lake (Figure
222 4). Acoustic penetration is limited in transects A and E by coarser sediments proximal
223 to river fan-deltas across Cariboo Lake (see triangle symbols in Figure 3 for fan-
224 delta locations). Acoustic signal penetration, resolution and distinctive acoustic layering
225 improves significantly along the thalweg of the lake bottom away from the main Cariboo
226 River delta and in cross-lake transects more distal from the valley-side fan-deltas. **The**
227 **diagonal lines across all panels (cross-hatching) in Figure 4 is observed over most**
228 **of the acoustic record due to errant electrical interference from the research vessel**
229 **that could not be resolved.** However, the interference does not affect the overall quality
230 of the acoustic results in the six selected transects (Figure 4, A-F).

231 Transect A, one kilometer southwest of the headwater Cariboo River delta, has a strong
232 acoustic reflector at the sediment-water interface indicating the presence of coarser-
233 grained material on the lakebed (Figure 4, A). Grab samples on this transect show a
234 high fraction of sandy materials which act as an acoustic mask limiting the penetration
235 of the acoustic signal to a depth of 1-2 m. An acoustic multiple (echo) is observed 45 m
236 below the sediment surface caused by the limited penetration at the surface (Figure 4, A
237 - i). Acoustically penetrable, well-layered sediment is observed 3.5 km from the Cariboo
238 River delta in transect B (Figure 4, B). This site is proximal to long core V1. Acoustic
239 reflectors with 1-2 m separation lie conformably over a hummocky basement which is
240 observed on the south side of the transect (Figure 4, B - i). The acoustic basement drops
241 off below the observable record near the south channel-like depression. Well structured
242 layering extends across the south side of the transect but pinches out towards the north
243 shore (Figure 4, B, C & D). On the south side of transect B, the thickness of the well
244 structured layering ranges from 10 to 20 m. Underlying the layered sediments is a more
245 massively layered facies which ranges from 12 to 25 m thick before the record is cut off
246 **below the maximum depth of the record of 80 m.**

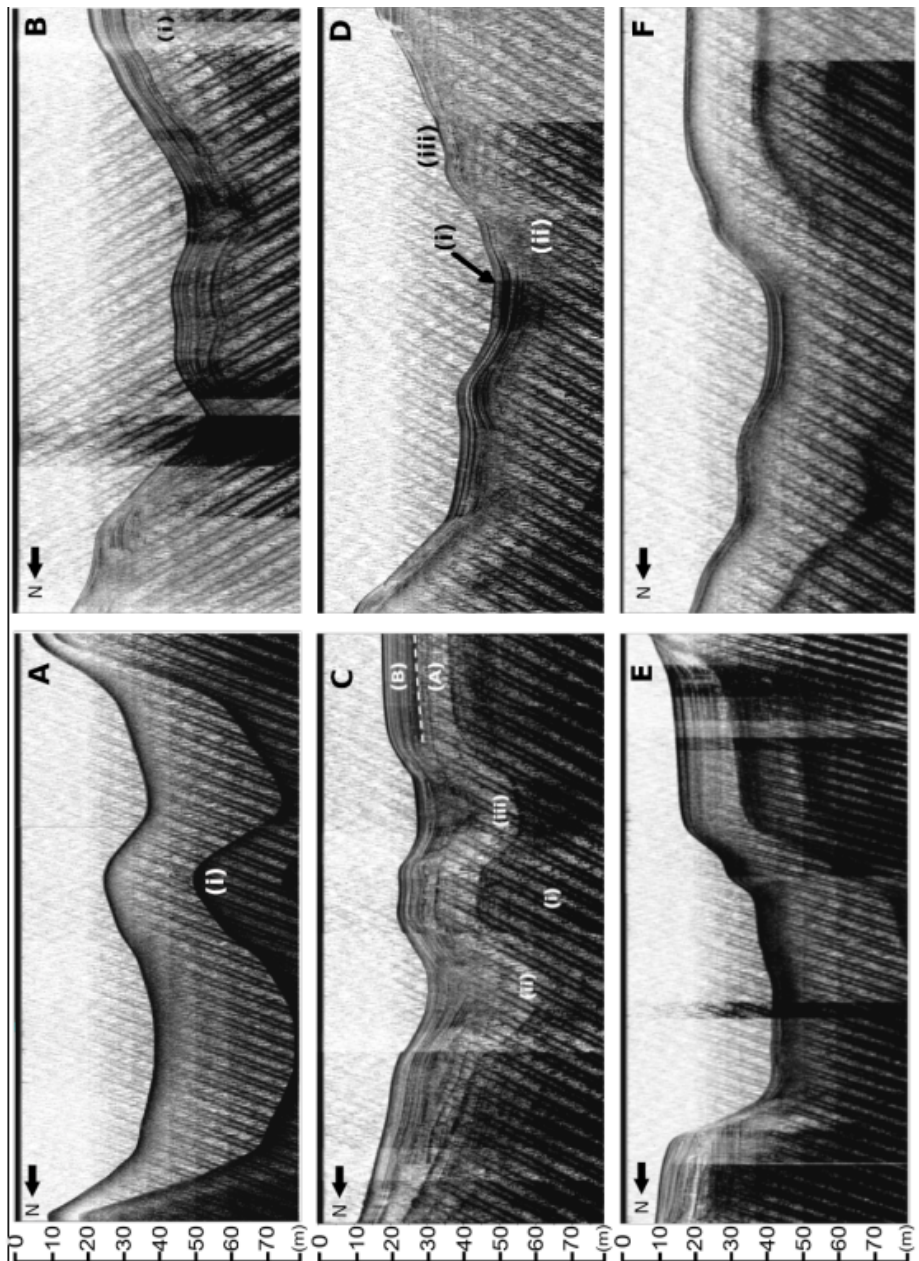


Figure 4. Panel of six selected sub-bottom acoustic transects A, B, C, D, E, and F. The left-hand side of each transect corresponds to the north-shore of the lake, see Figure 2 for location of each transect. Transect A and B: Acoustic echo (multiple) is denoted by (i). Transect C: (i) denotes inferred bedrock or coarse late-glacial material. (ii) and (iii) are v-notch scour channels. (A) and (B) are sediment facies. Transect D: Scour channels are denoted by (i) and (ii). Slumping is observed at (iii).

Acoustic penetration increases 4.5 km from the Cariboo River delta at transect C (Figure 4, C). The acoustic record along this transect reaches a maximum sediment thickness of 35 m in two troughs, the maximum thickness of surficial sediments observed across Cariboo Lake in this study. The acoustic basement is considered to be either bedrock or coarse-grained glacial sediment from the Last Glacial Maximum (Figure 4, C – i). Two sediment facies are observed across this transect based on geometry and the strength and continuity of reflectors. Some disruption of these facies is caused by slumping of side slopes (e.g. north end of transect C). The lower unit, facies A, has a thickness of ~12 m along undisturbed sections (Figure 4, C) and is more massive to weakly acoustically layered. The contact with overlying sediment above facies A appears to be conformable at the south end and middle of the transect but unconformable in other places. The unconformities are most apparent in the two sharp crested v-notch channels at the middle of the transect. These channels are a continuation of those noted in transect B. These are inferred to be scour channels formed by erosive, higher energy, turbidity currents that probably date to deglaciation of the lake basin. The lack of numerous layers and generally lighter grey tone in facies A indicates a somewhat higher energy and more rapid deposition of coarser lacustrine sediment. Facies B begins with high-amplitude parallel reflectors with 2-3 m separation and conforms well with facies A below (Figure 4, C). Facies B has a thickness of ~10 m along undisturbed sections and deepens to a maximum of 13 m within the scour channels (Figure 4, C - ii & iii). The strength of reflectors in facies B are stronger and more numerous than those in facies A indicating more frequent events of lower overall magnitude during this time. The strength of reflectors gradually decreases moving upwards and spacing thins to sub metre thickness near the surface. The gradual decrease in reflectance is interrupted by a strong reflector at the top of facies B along the sediment-water interface.

The two buried troughs in transect C (Figure 4, C - ii, iii) are significant and best expressed in this area of the lake. The north trough (ii) appears to be a depression that was continuously infilled by facies A and then B. Hence it most likely represents an older pre-existing feature. The sediments in the southern trough (iii) are interesting in that a wedge of sediment infill seems to be an unconformable deposit with both facies B below and facies A above. **This wedge of sediment is observed in Figure 4 (see above label C-iii) characterized by a deepening of facies B and darker in color than facies A.** It is likely that an erosional channel developed after or in the later stages of facies A deposition which infilled the wedge. Sedimentation of the wedge was then truncated by the onset of the facies B sediment. While the two troughs might have been active at the

same time during deglaciation, only the southern trough was reactivated at a later time and infilled with sediment prior to the onset of facies B deposition.

Transect D, to the northeast of the Frank Creek delta has well-layered sediments in the top 5-10 m and transitions to poor acoustic penetration below this (Figure 4, D). The parallel reflectors observed in the uppermost sediment layers of transect D have a thickness of 2-3 m and have a higher amplitude compared to facies B in transect C. Some slumping of sidewall sediments is observed on the south sidewall (Figure 4, D).

Southwest of the Frank Creek fan-delta, acoustic reflectors along transect E show a decline in reflectance and a decrease in layer thickness to < 1 m. Acoustic masking from coarse grained sediment occurs at depths of 2-4 m along the south margin (Figure 4, E). Total sediment thickness of finer, acoustically well-layered material along the north bench is significant approaching 10 m. The profile suggests that much of the suspended sediment transported from the upper lake does not make it past the shallow lake depths (< 20 m) of the sill at the Frank Creek fan-delta apart from the northern most part of the transect. Coarser sediment from the Frank Creek fan-delta dominates the south side of the transect and fine sediment deposition is restricted, or forced, to the north side.

Similar to the Frank Creek fan-delta, the very shallow sill of less than 2 m opposite the Keithley Creek prograding fan-delta significantly reduces sediment connectivity to the main Cariboo Lake basin (see triangle proximal to Keithley Creek in Figure 3). Transect F, located close to the centre of the Keithley Creek sub-basin shows a maximum observable sediment thickness of 4 m concentrated in the basin thalweg (Figure 4). Below this there is acoustic masking by coarser sediment. The acoustic reflectors within the top 4 m of transect F are acoustically penetrable, well layered and are conformable to the basin morphology. These reflectors are of higher amplitude compared to those in transect E and are thicker at 1-2 m. This suggests that significant amounts of coarse-grained sediments are found in this part of the lake, likely originating from the high energy Keithley Creek drainage basin. Fine fraction sediments from the main Cariboo Lake are expected to make up a small percentage as transport into this sub-basin is limited by up-lake storage, filtering and hypopycnal overpassing.

311 Spatial Trends in Surficial Sediment

312 Twenty surficial sediment cores ranging from 6-12 cm thick were analyzed for grain
313 size, laminae thickness, and organic content. These samples were collected following
314 a longitudinal transect down Cariboo Lake and indicate how sediment flux varies with
315 distance from the Cariboo River delta (see Figure 3, for sampling locations). **The percent**

of sand-sized sediments follows an exponential decline with distance down-lake starting at 60.8% sand proximal to the Cariboo River delta and reaching a low of 0.15%, 5.2 km km from the Cariboo River delta (Figure 5, A). The D₅₀ grain size also follows a steep decline from 89.9 µm, 300 m from the delta, to 31.3 µm 550 m from the Cariboo River delta (Figure 5, B). The decline in D₉₀ grain size follows a more pronounced decline, while the D₁₀ remains largely unchanged. This suggests that larger sand-sized sediments (63-2000 µm) are sensitive to distance from fan deltas, while smaller silt-sized (2-63 µm) and clay-sized (0.01-2 µm) sediments are less sensitive. At distances greater than 2 km from the Cariboo River delta the fraction of silt-sized sediments remains at over 80%, aside from core E16 which is near the Frank Creek fan-delta. The highest percent of silt (86.5-89.6%) and clay (9.3-14.4%) sized sediments are observed between 3 and 6.5 km from the Cariboo River delta, proximal to the long core sampling locations. Near to the Frank Creek fan-delta the D₅₀ grain size nearly doubles in size from 7.92 µm at 6.4 km to 15.1 µm at 7.35 km from the Cariboo River delta. In the Keithley Creek sub-basin the D₅₀ grain size has an average grain size of 15.9 µm (n = 3) and the composition of sediment is 4.0% clay, 85.8% silt, and 10.2% sand (Figure 5, A, B).

Proximal to the Cariboo River delta (< 500 m) the structure of the surficial sediments exhibits massive layering, erosive contacts and the fraction of sand grains in these samples is greater than 60%. A sand-bed with a thickness of 1 cm is observed in the bulk sample closest to the Cariboo River delta (Figure 6, A). In the main Cariboo River basin, core E13 had the most distinct laminations and was taken 5.24 km from the Cariboo River delta, proximal to long core V2, in the deepest part at a depth of 40 m. Sediment here shows rhythmic lamination (Figure 6, B).

Sediment cores E9-E15 and E18-E20, retrieved from areas in Cariboo Lake that are distal from river deltas and have lake depths of 30-50 m, have a high fraction of silt and clay sediment and exhibit a sequence of fine-grained dark layers followed by coarse-grained light layers (Figure 6, B & C). The sediment stratigraphy observed within cores E9-E15 and E18-E20 is similar to annual laminations (also called varves) observed in many other lakes (Cockburn and Lamoureux, 2008; Zolitschka et al., 2015; Heideman et al., 2015; Hodder et al., 2006; Desloges, 1999) that have sufficient seasonal variation in river discharge and lake stratification. In the Cariboo Lake basin, winter low flows, lake-ice cover, and lake stratification reduce the velocity of lake currents and contribute to the deposition of fine-grained sediments on the lake bottom. During the spring nival high flows, coarser-grained sediments are

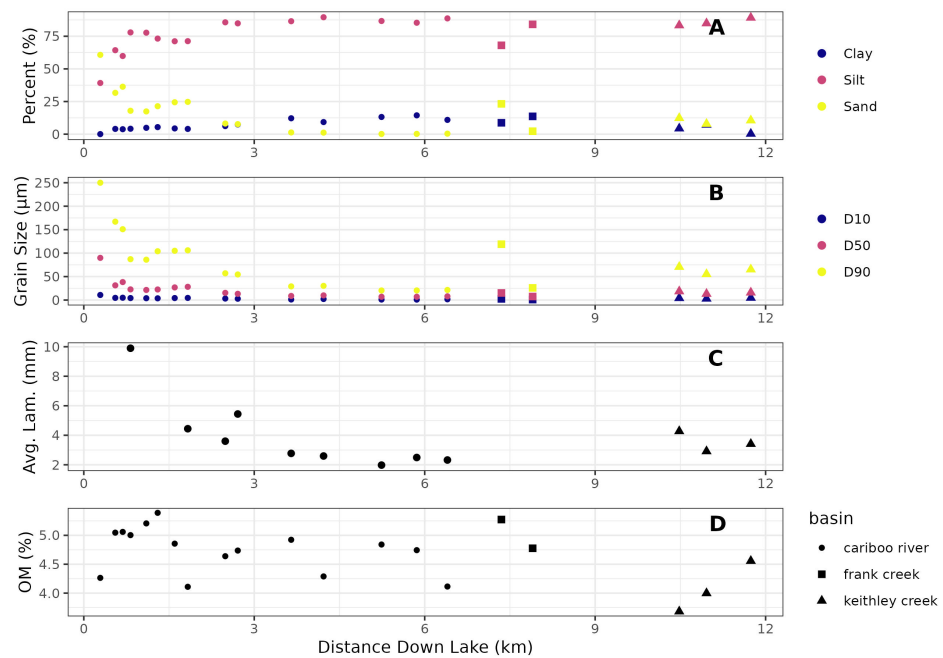


Figure 5. Sediment characteristics from the Ekman surficial bulk samples with distance down lake from the Cariboo River input to Cariboo Lake. Top panel A is the percent clay (0.01 - 2) µm, silt (2 - 63) µm, and sand grains (63 - 2000) µm, panel B is the D 10 , D 50 , and D 90 (µm) grain size, panel C is the mean laminae thickness (mm), and the bottom panel D is percent organic matter content (OM).

351 deposited as a result of higher energy lake currents. Additional deposits of coarse-
 352 grained sediment also may result due to abnormally high discharge events such as
 353 large rain or snow-melt events and/or turbidite beds due to delta collapse (Sabatier
 354 et al., 2022). Coastal lakes in western Canada that are frequented by large rain
 355 storms and mid-winter melt events lead to multiple laminae couplets deposited in
 356 a given year (Menounos and Clague, 2008). However, the distinct spring snowmelt-
 357 dominant hydrological regime of the Cariboo Lake watershed shown in Figure 2
 358 suggests the deposit of multiple coarse-grained laminae in one year is rare. Coarse-
 359 grained deposits are still possible in Cariboo Lake due to turbidite beds from delta
 360 slumping/foreset failures however these turbidite beds are only observed in Ekman
 361 cores proximal to Cariboo Lake river deltas (e.g. Figure 6, A). While the sediment
 362 stratigraphy of Ekman cores E9-E15 and E18-E20 resemble varves, further analysis
 363 of the Cariboo Lake long-cores and C14 chronology is required to confirm this.

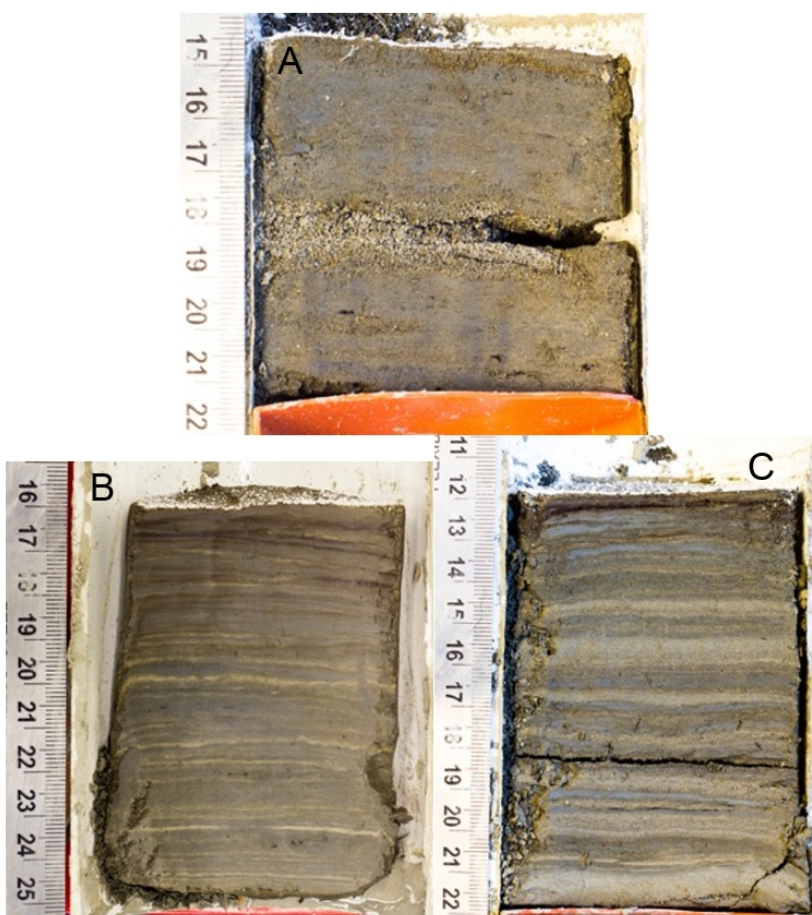


Figure 6. Selected surficial Ekman sediment core photographs. A (E1) is proximal to the Cariboo River delta (0.3 km down lake). B (E13) was retrieved from the second deepest basin in the lake in the Cariboo River basin (5.24 km down lake). C (E18) was retrieved from the Keithley Creek sub-basin (29.53 km down lake).

The thickness of sediment laminae couplets within cores E9-E15 and E18-E20 demonstrate a gradual decreasing trend with distance down-lake from the Cariboo River delta (Figure 5, B). This suggests the Cariboo River is the main source of sediment into Cariboo Lake as sediment flux typically declines with distance from the primary sediment source. Maximum couplet thickness has an average of 4.7 mm ($n = 6$) in the Cariboo River basin and 7.9 mm ($n = 3$) in the Keithley Creek sub-basin. In the Cariboo River basin, maximum couplet thickness decreases by 0.62 mm/km and by 2.17 mm/km in the

371 Keithley Creek sub-basin with distance down-lake (Figure 5, B). The decline in thickness
372 is more rapid in the Keithley Creek sub-basin is likely due to additional local inputs of
373 coarser grained sediment coming from the Keithley Creek tributary.

374 Trends in percent organic matter (OM) of surficial sediment cores were not found
375 to exhibit systematic patterns with distance down-lake (Figure 5, C). **The lowest OM**
376 **values were observed in the Keithley Creek sub-basin and suggest higher levels of**
377 **clastic sediment yield in this basin which dilutes the OM signal.**

378 The results from particle size, laminae thickness, and percent organics **supports the**
379 **hypothesis that** sediment delivered from the main Cariboo River is the primary source
380 of sediment to Cariboo Lake. Massive layering of sediment and coarse-grained particle
381 sizes are limited to areas proximal to Pine Creek, Frank Creek and Keithley Creek deltas
382 where localized turbidity currents are active. Outside of these areas, where turbidity
383 currents and bedload transport processes are reduced, the sediment in Cariboo Lake is
384 largely comprised of rhythmically laminated silt and clay sediments likely transported
385 primarily through suspended sediment processes from the main Cariboo River. In the
386 Keithley Creek sub-basin grain size and laminae structures are larger in size than those
387 observed in the main Cariboo River basin suggesting local sediment inputs from the
388 Keithley Creek are significant (Figure 6, C).

389 *Sediment Accumulation Chronology*

390 Four vibra sediment cores, ranging from 2 – 4 m in length, were retrieved from the
391 deepest portions of Cariboo Lake (Figure 3). Cores V1 (3 m) and V2 (4 m) in the main
392 Cariboo River basin were selected for detailed analysis as these two cores had organic
393 material for AMS radiocarbon dating, and their sediment stratigraphy was well preserved.
394 The chronology of the two cores is provided by a small number of AMS radiocarbon
395 dates and laminae counting. **A search for volcanic tephra was made through careful**
396 **magnified inspection of visual color changes. None were found using this method.**
397 **Westgate (1977), Hallett et al. (1997) and Maurer et al. (2012) indicate that this area**
398 **of British Columbia has had episodic volcanic ash inputs from significant eruptions**
399 **that predate 2100 years BP but nothing since. The chronology of the Cariboo**
400 **Lake core records of grain size, varve thickness, and organic content demonstrate**
401 **patterns in sediment delivery to Cariboo Lake over approximately the past 2000**
402 **years.**

403 **Chronology** Organic material for dating in the clastic dominated cores was extremely
 404 limited. AMS radiocarbon dates obtained for cores V1 and V2 are presented in Table
 405 1 and provide limited temporal control and evidence of sediment accumulation rates
 406 for the long cores. A small twig from V1 at 343 cm and combination of two separate
 407 organic pieces which were combined into one sample at V2, with an average depth of
 408 281 cm, yielding a calibrated (Reimer et al., 2013) two-sigma date range of 1820-1918
 409 cal BP and 1895-2043 cal BP respectively. Figure 7 shows the ^{14}C chronology for V1 and
 410 V2 compared to the laminae couplet chronologies for E13, V1, and V2. The ^{14}C dates
 411 from samples V1 and V2 yield accumulation rates (**depth of sample divided by age of**
 412 **sample**) of $1.76 \pm 0.05 \text{ mm yr}^{-1}$ and $1.37 \pm 0.05 \text{ mm yr}^{-1}$ respectively.

Table 1. Cariboo Lake chronologic control points.

Core Name	Type	Depth (cm)	^{14}C (yr BP)	^{14}C 1 σ	2 σ age range (cal BP)	Median age (cal BP)
V1	Surface	0	NA	NA	NA	-67
V1	14C	343	1913	21	1820-1918	1859
V2	Surface	0	NA	NA	NA	-67
V2	14C	281	2020	28	1895-2043	1968

413 Ekman surficial core 13 (E13), shown in Figure 7, is most proximal to the V2 long
 414 core (see Figure 3) and exhibits similar sediment accumulation compared to the ^{14}C
 415 and laminae chronology of V2. The light-dark couplets in E13, shown in Figure 6, are
 416 similar to annual deposits noted in dozens of other lakes throughout BC (e.g. Hodder
 417 et al., 2006). Therefore, the couplets within the Ekman cores are assumed to closely
 418 approximate varves, in which case E13 exhibits an average accumulation rate of $1.98 \pm$
 419 0.19 mm yr^{-1} . Higher accumulation rates are expected for the Ekman samples as they are
 420 not subjected to the same level of compaction as is deeper sediment in the long cores.
 421 The consistency of the E13 inferred accumulation rate when compared with two of the
 422 AMS dates from the V1 and V2 cores (Figure 7) are additional evidence of the varved
 423 nature of the sediment record.

424 **By comparison with nearby lakes**, accumulation rates in areas proximal to river
 425 inputs in nearby Quesnel Lake were measured to be about 0.72 mm yr^{-1} (see Figure 9
 426 in Gilbert and Desloges (2012)). Sediment inputs are expected to be lower in Quesnel
 427 Lake compared to Cariboo Lake, with more arid and less glaciated portions of the
 428 Quesnel Lake watershed contributing to that lower rate. The AMS accumulation rates

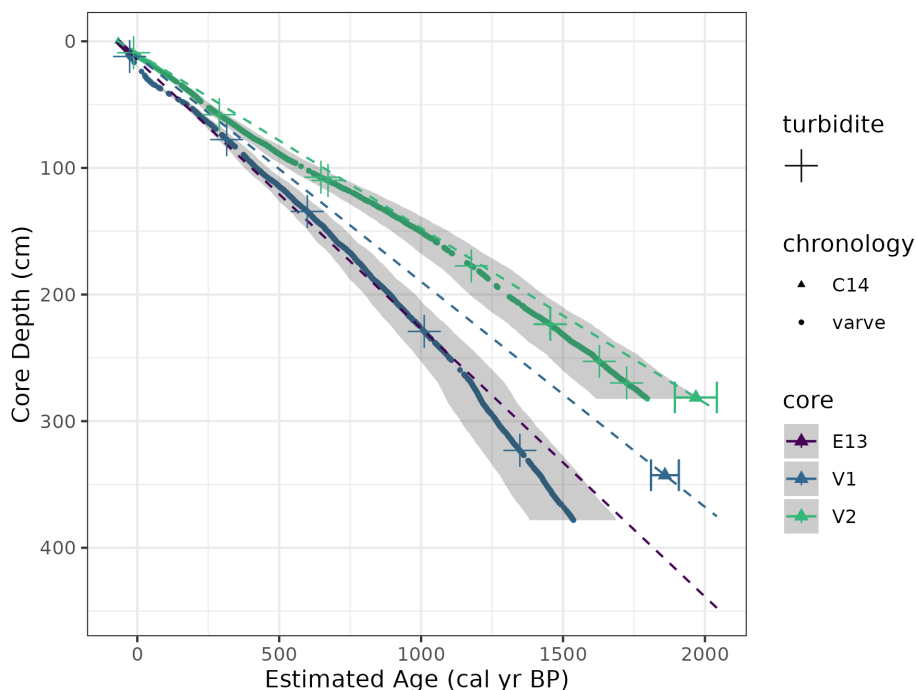


Figure 7. Cumulative sediment accumulation rates for cores V1 and V2 using the median calibrated ^{14}C AMS dates and lamanae couplet counting and thicknesses measurements. The error bars on the ^{14}C dates are the two-sigma uncertainty range and the grey shading around the varve points is the 10% counting error. Gaps between the varve chronology (points) denote periods that had indiscernible varves. The accumulation rate for the Ekman surficial core which has a maximum observed depth of 9 cm has been extrapolated using linear interpolation.

of $1.76 \pm 0.05 \text{ mm yr}^{-1}$ and $1.37 \pm 0.05 \text{ mm yr}^{-1}$ in Cariboo Lake are as expected for a smaller watershed with a higher fraction of glacier cover compared to Quesnel Lake. The AMS radiocarbon dates from samples V1 and V2 provide an important control when interpreting the inferred temporal pattern of sediment inputs to Cariboo Lake.

Three distinct sediment facies were observed in both V1 and V2: discernible couplets, indiscernible couplets (disturbed facies) and graded turbidite events. The similarity in couplet structure and thickness between cores V1 and V2 and hydrology of Cariboo Lake strongly suggested these are varves. This interpretation is also supported by the two AMS radiocarbon dated samples from cores V1 and V2 which corresponded reasonably well with the couplet count chronology at the same depth (Figure 7). A small difference

439 between the two chronologies was expected due uncertainties with counting errors.
440 The uncertainty of the laminae counting method is inferred from Ekman surface
441 cores by counting laminae down to a common specified depth of 5 cm for three
442 Ekman cores (E12, E13, E14 - see Figure 3 for locations proximal to V1 and V2).
443 The Ekman laminae counting analysis resulted in an uncertainty estimate of the
444 counting method of about 10% or 1 miscounted varve per 10 years. This counting
445 error of 10% is higher than the varve counting error of 0.7% in Menounos and
446 Clague (2008) and 0.7-6% in Zolitschka (1991). In Menounos and Clague (2008)
447 and Zolitschka (1991) varves were identified using thin sections and may have
448 contributed to a more accurate chronology. The varve contacts observed in Cariboo
449 Lake were strong and there is reasonable confidence in counting. Missing varves
450 may have occurred if the spring nival high flows did not deliver a coarse-grained
451 laminae and false varves may occur if multiple high flows are observed in a given
452 year. However, the consistent nival flows of this basin shown in Figure 2 suggest
453 multiple high flow events are rare. This hypothesis is also supported by Figure 7
454 which shows a negative bias of the varve chronology compared to the calibrated ^{14}C
455 age-depth model and suggests that missing varves may be a larger source of error
456 than false varves.

457 Instantaneously deposited (event-based) turbidites were identified if laminae/beds had
458 D_{50} grain size greater than 3 standard deviations from the mean and/or thickness greater
459 than 6 standard deviations for V1 and 2 standard deviations for V2 from the mean. Figure
460 8 examples show the difference in regular laminae compared to an event-based turbidite
461 bed. Turbidite beds observed in V1 and V2 were well defined and graded (see Figure
462 8, d). These turbidite beds are similar in structure to those described in Sabatier et al.
463 (2022) as originating from a flood, glacial lake outburst flood, or delta collapse event.
464 Since the Cariboo River upstream of Cariboo Lake is filtered by headwater proglacial
465 lakes, it is more likely the turbidite beds at the distal V1 and V2 site are from localized
466 sidewall tributary floods. Collapse of the foreslope of an oversteepened Cariboo delta is
467 also possible.

468 Where possible the thickness, grain size statistics, and percent organic matter (OM)
469 were analyzed for each event layer. The turbidite bed grain size, OM, and thickness
470 shown in Table 2 illustrates the high sediment flux during these events compared to
471 the regular, annually occurring couplets. The composition of sediment grains within
472 the event-based layers were all characterized by a coarser single mode with less than
473 0.01% clay, over 98% silt and less than 1% sand. The grain size distribution for the

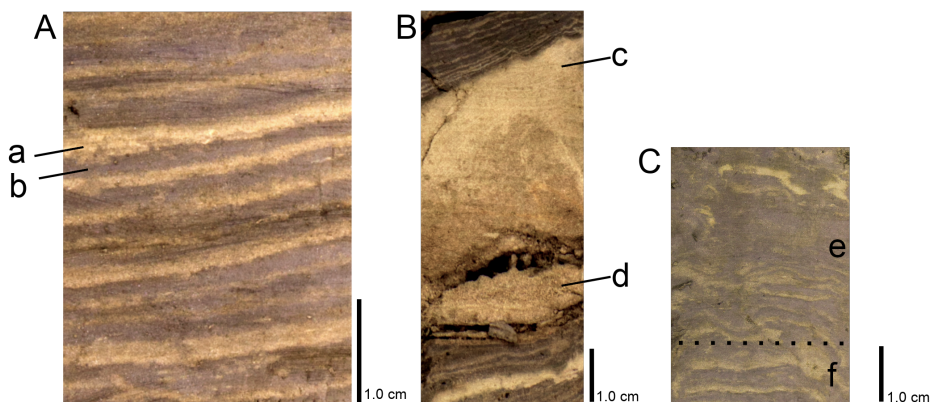


Figure 8. A. Example of regular laminae from V1 at a depth of 360 cm. B. a graded event-based turbidite bed from V2 at a depth of 230 cm. Features labeled within this figure include: 'a' high flow spring/summer freshet laminae, 'b' low flow winter laminae, 'c' top of the turbidite bed, and 'd' the bottom of the turbidite bed. C. shows massive beds 'e' over more distinct laminations 'f'.

regular couplet sediments is characterized by a bi-modal distribution with an average composition of 16% clay, 83% silt, and less than 1% sand. Figure 9 shows that some event layers are coincident in time between V1 and V2. Since each of the event-based layers contain sediment deposited over a single, potentially localized event, they were removed from subsequent trend analyses of varve thickness, grain size, and percent organics.

Table 2. Sediment characteristics of regular laminae 'Couplet (varve)' compared to couples classified as turbidite beds 'Events' for V1 and V2. The 'Couplet (varve)' is the mean sediment characteristic for all regular laminae couples. The 'Event mean' is the mean sediment characteristic value for couples classified as events, 'Event sd' is the standard deviation, and 'Event n' is the number of turbidite beds.

core	metric	Couplet (varve)	Event		
		mean	mean	Event sd	Event n
V1	D ₅₀ (µm)	7.64	9.68	0.80	5
V2	D ₅₀ (µm)	6.35	16.20	9.40	6
V1	OM (%)	4.75	4.67	0.53	3
V2	OM (%)	4.71	2.86	0.94	4
V1	Avg. Thickness (mm)	2.39	10.32	4.24	5

core	metric	Couplet (varve)	Event		
		mean	mean	Event sd	Event n
V2	Avg. Thickness (mm)	1.51	9.58	14.12	9

The varve-based chronology is based on the counting of discernible couplets with graded turbidite facies removed. **Indiscernible couplets in the disturbed-massive units makes interpreting the time elapsed over each of these units difficult (see Figure 8 C).** To compensate for the depth intervals associated with the disturbed sections, a 30-year moving average of sediment accumulation rates from immediately above and below the disturbed sections were used to interpolate accumulation rates over each facies (see method described in Menounos et al., 2008). For core V1, laminae couplets were counted down to a core depth of 343 cm, where the AMS radiocarbon organic material was retrieved. **This resulted in a V1 couplet-derived age estimated of 1419 ± 142 varve BP compared to the two-sigma calibrated ^{14}C age range of 1820-1918 cal BP.** For core V2 a date of 1792 ± 180 varve BP was estimated by couplet counting down to a core depth of 281 cm which matches more closely with two-sigma calibrated ^{14}C age range of 1895-2043 cal BP. The better alignment between the couplet counting age and the AMS derived age in V2 can be attributed to the higher degree of core disturbance in V1 compared to V2. Disturbed sections that had indiscernible couplets may have resulted in the undercounting within core V1. Still, based on the relatively close agreement between the AMS radiocarbon dated organic material and couplet counting, laminae couplets in V1 and V2 are considered to be deposited annually. Alignment closer than the observed offset at V1 was not expected due to the uncertainty in the ^{14}C and varve based chronology. The varve estimate at V2 is nearly within the uncertainty range of the calibrated ^{14}C age and therefore shows good agreement between the varve and ^{14}C chronologies.

The basal age for each core is estimated using both the varve counting method and using a linear interpolation to extrapolate the ^{14}C chronology. The basal age of V1 at 378 cm is approximately 1537 ± 154 varve yr BP based on the varve chronology and the two-sigma calibrated ^{14}C range is 2016-2124 cal BP. The basal age of V2 at 282 cm is about 1797 ± 180 varve yr BP based on the varve chronology and the two-sigma calibrated ^{14}C range is 1902-2051 cal BP. The closer alignment of the ^{14}C and varve chronology at V2 gives greater confidence in the timing of Holocene sedimentation patterns for this core. While V1 has a greater spread between the

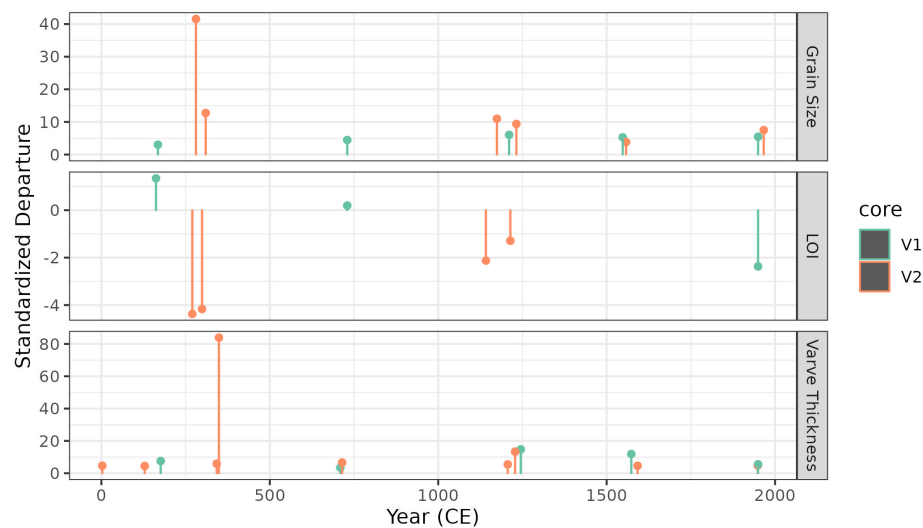


Figure 9. Timing and Standardized Departures of turbidite thickness, grain size, and OM for V1 and V2. Year (CE) is the estimated year using linear interpolation from the AMS radiocarbon dates.

509 two chronology methods, we believe both cores are valid estimates of late Holocene
 510 sediment accumulation patterns in Cariboo Lake.

511 *Sediment Laminae Statistics* A time series of varve thickness (as standardized
 512 departures) is presented in Figure 10, using only discernible couplets. Event-based
 513 turbidites have been removed and indiscernible facies are represented as gaps. The
 514 chronology for this time series was derived using a linear interpolation from the
 515 median calibrated ^{14}C date of each core (Table 1). The mean varve thickness for V1
 516 is 2.4 mm and for V2 is 1.5 mm. Thicker varves are expected at V1 due to its closer
 517 proximity to the Cariboo River delta. This is also supported by the thicker varves
 518 observed in core E11 (proximal to V1) compared to E13 (proximal to V2) of 2.8 mm
 519 to 2.0 mm respectively. The time series of varve thickness measured from V1 and
 520 V2 and illustrates trends in suspended sediment delivery to Cariboo Lake (Figure
 521 10). The measured couplet thicknesses in the two cores are plotted as standardized
 522 departures to facilitate comparison between the two cores. In each plot a 30-year
 523 moving average with a 1-year time step is plotted in black to emphasize decadal
 524 to centennial patterns in accumulation rate departures. The 30-year average varve
 525 thickness remains above average from 0 to 750 CE, for both V1 and V2, with a

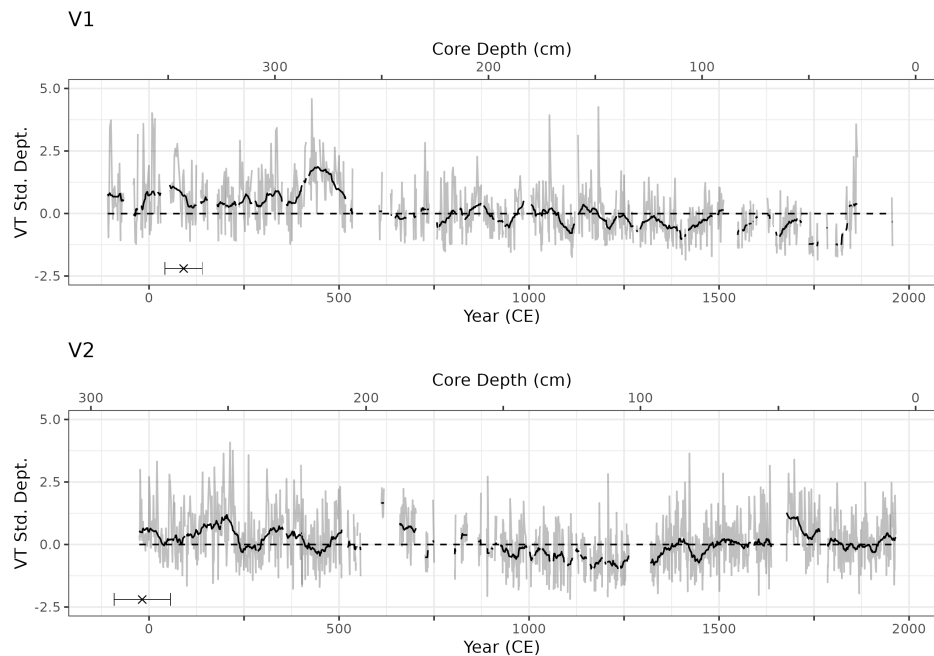


Figure 10. Standardized departure from the mean varve thickness (VT) for cores V1 and V2. Events are removed from the record and disturbed facies are shown as blank gaps in the record. The gap width of disturbed facies was calculated using a linear interpolation from the AMS radiocarbon dates. The gray lines represent measured varve thickness at couplet (annual) resolution where available, the black line is a 30-year moving average. Gaps correspond to portions of the core that did not have discernible varves. The bottom axes, labeled Year (CE), was estimated using linear interpolation from the median calibrated ^{14}C age. Lamination counting in V1 was not possible beyond the estimated date of 1900 CE and beyond 1970 CE in V2. The black X's on the bottom graph of V1 and V2 denote the AMS radiocarbon age (\pm dating error) and depth of the respective sample.

stronger signal observed for V1 which is closer to the main Cariboo River outlet. Below average varve thickness is observed at both V1 and V2 from 750-1600 CE. After 1600 CE, trends in varve thickness between the two cores depart, with V2 above average during the Little Ice Age and V1 remains below average. Sub-centennial trends are not reported due to the coarse temporal control for both V1 and V2.

Grain Size The mean D_{50} grain size is $7.6 \pm 0.01 \mu\text{m}$ at V1 compared to $6.3 \pm 0.01 \mu\text{m}$ at V2. The larger grain size and varve thickness at V1 compared to V2 is consistent with the spatial trends in sediment delivery observed from the Ekman cores. While based on a

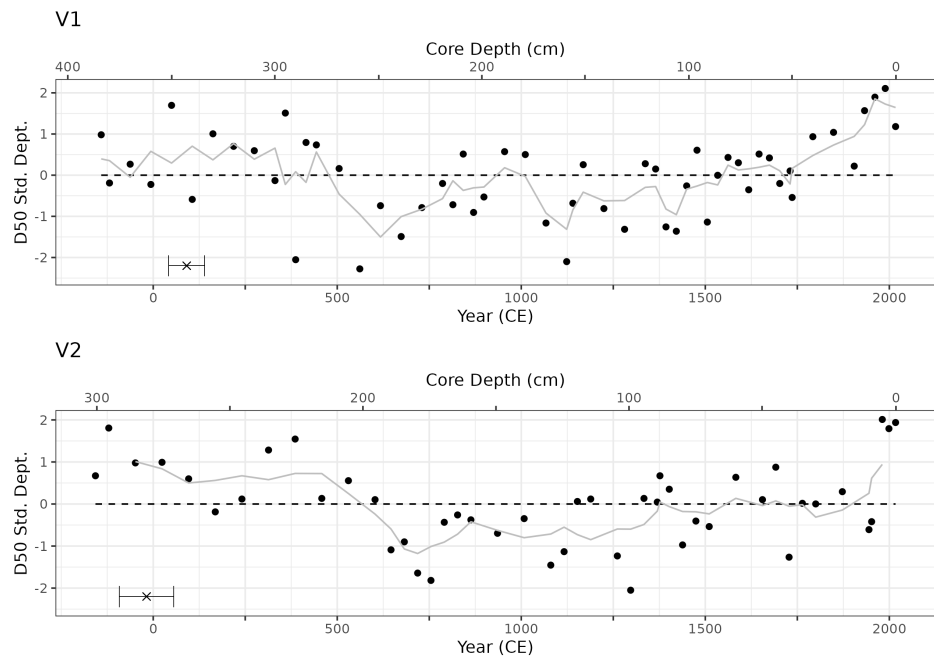


Figure 11. Standardized departure from the mean D₅₀ grain size for cores V1 and V2. The black points represent D₅₀ grain size at 5 - 10 cm intervals and the gray line is the 3 sample (125 year) moving average. The top axes, labeled Year (CE), was estimated using linear interpolation from the median calibrated ¹⁴C age. The black X's on the bottom graph of V1 and V2 denote the AMS radiocarbon age (\pm dating error) and depth of the respective sample.

535 limited number of measurements compared to the varve thickness analysis, the temporal
 536 pattern in standardized departures of D₅₀ grain size between the two cores shows a
 537 consistent pattern (Figure 11). Both V1 and V2 have above average grain size between 0
 538 to 700 CE and below average from 700 to 1500 CE. After 1500 CE, grain size follows an
 539 increasing trend with average to above average grain size. V1 shows an earlier increase in
 540 grain size compared to V2. While couplet thickness does not increase substantially over
 541 the LIA interval, gain size does. Overall, grain size fluctuations at a temporal resolution
 542 of about 100-years shows good correspondence between the two cores over the last 2000
 543 years.

544 **Organic Matter** The average percent organic matter (OM) at V1 and V2 is similar at
 545 4.76% and 4.80%, respectively, suggesting that the flux of allochthonous organic material
 546 to the core locations is not dependent on distance from the main Cariboo River as it
 547 is easily transported through the lake due to low density. This is also supported by the

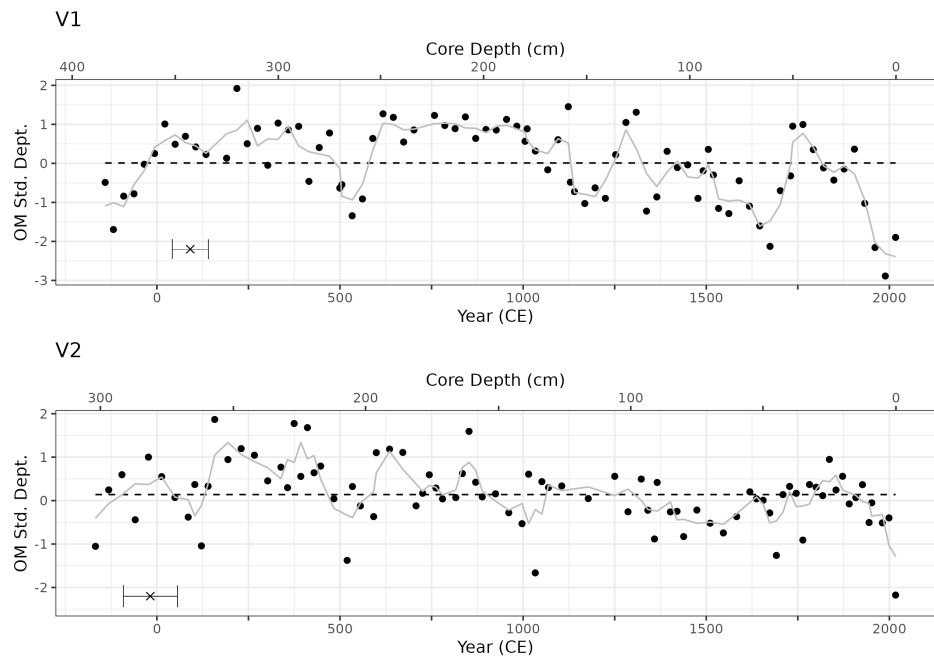


Figure 12. Standardized departure from the mean percent organic matter (OM) for cores V1 and V2. The black points represent percent OM at 2.5 - 5 cm intervals and the gray line is the 3 sample (75 year) moving average. The top axes, labeledled Year (CE), was estimated using linear interpolation from the median calibrated ^{14}C age. The black X's on the bottom graph of V1 and V2 denote the AMS radiocarbon age (\pm dating error) and depth of the respective sample.

Ekman OM spatial analysis, where a systematic down-lake relationship was not observed (Figure 5, C). Figure 12 shows the percent OM for both V1 and V2. Higher levels of organic content are shown in V1 and V2 from 0-1000 CE and mostly below average from 1000-2000 CE. Specific periods of above average OM for V1 occur around CE 50-500, 650-1150, around 1300 and 1750-1850. OM in V2 matches above average values in the interval CE 250-550 and 650-950. During the last 100 years both cores show a persistent decline in OM which could be attributed to a relative increase in sediment delivery to Cariboo Lake suggested by the increase in D_{50} and varve thickness. As **glaciers declined from peak LIA extents around 1750 CE (Leonard, 1997; Luckman, 2000)**, an increase in soil development, vegetation growth and subsequent bank stability is expected which may also contribute to a decline in OM as organic content is locked up as needleleaf coniferous forest.

560 Discussion

561 Cariboo Lake was selected to test the utility of moderate sized glacier-fed lakes as
562 archives of accessible long-term and high-resolution sediment input variability. Evidence
563 of late Pleistocene deglaciation in the Cariboo Lake region is provided by coarse temporal
564 resolution sub-bottom acoustic results. A maximum deglacial sediment thickness of
565 ~35 m puts Cariboo Lake in the middle to lower range of Holocene sediment inputs
566 in Canadian Cordilleran lakes (see detailed discussion in [Gilbert and Desloges, 2012](#)).
567 The study of smaller Mud Lake, in the Rocky Mountains to the east of Cariboo Lake
568 (Figure 1 – inset) was evaluated by [Hodder et al. \(2006\)](#), who found the early phases of
569 deglaciation and lake sediment infill started just prior to 9.6 ka BP. [Gilbert and Desloges](#)
570 ([2012](#)) indicate deglaciation of the north and west arms of nearby Quesnel Lake was
571 likely complete by 8.6 ka BP. [Menounos et al. \(2009\)](#) pointed to the deglaciation of
572 most of the Cordilleran ice sheet before 10.5 ka BP. The Cariboo Lake acoustic results
573 contribute to this regional record however the inferred bottom dates present uncertainty
574 in the actual timing.

575 Unlike many other deglacial sediment packages in Canadian Cordilleran lakes, the
576 sediment infill in Cariboo Lake has been subject to deep trenching during deglaciation
577 and the early Holocene (Figure 3c). The troughs, with sediment infills occurring at
578 different times, suggest the presence of highly erosive but intermittent bottom currents
579 during deglaciation and into the very earliest Holocene. Energetic flow of cold sediment-
580 rich meltwater flow would be required suggesting proximity of an actively retreating
581 valley glacier. The absence of lower elevations moraines in the valley upstream of
582 Cariboo Lake might indicate rapidly retreating ice into headwater locations. However,
583 in general, moraines indicative of stagnant ice fronts in lower elevation settings are not
584 common elsewhere throughout much of the eastern Cordillera suggesting that valley
585 glacier development was limited ([Menounos et al., 2009](#)).

586 **In contemporary ice-proximal lakes with extensive coverage of active glaciers,
587 high accumulation rates have been observed to be between 0.5 m yr^{-1} ([Crookshanks
588 and Gilbert, 2008](#)) and as high as 1 m yr^{-1} ([Gilbert et al., 1997](#)).** Similar high
589 accumulation rates in the late-glacial are inferred to have occurred in Quesnel Lake
590 ([Gilbert and Desloges, 2012](#)), resulting in a thick pre-Holocene sediment package. This
591 evidence for high pre/early Holocene accumulation rates in Quesnel Lake from large
592 dynamic glaciers suggests that high accumulation rates are also likely for Cariboo Lake
593 during this time and is supported by the acoustic data presented here.

594 Two transects of sub-bottom acoustic records analyzed within Cariboo Lake
595 provide evidence of high sediment accumulation rates during the early Holocene.
596 Sub-bottom acoustic records from Transect B shown in Figure 4, which is proximal
597 to the V1 core, indicate an upward transition from massive-unlayered (Facies A) to
598 well-layered sediments (Facies B) at a depth of about 20 m. Assuming a maximum
599 Holocene sediment accumulation rate of approximate 1.9 mm yr^{-1} from V1, this
600 would put this transition at about 10.5 ka BP. Transect C, shown in Figure 4 is
601 located in-between cores V1 and V2, shows the transition of Facies A to B occurring
602 at a depth of around 15 m. Using a combined V1 and V2 average Holocene sediment
603 accumulation rate of 1.7 mm yr^{-1} in this region of the lake, puts the transition from
604 Facies A to B at around 9 ka BP for Transect C, slightly later than the Transect
605 B estimate. The massive structure of Facies A is inferred to be due to high rates
606 of sediment delivery as glaciers retreated upvalley during the early Holocene after
607 the formation of the deep trenches. The well-layered sediment of Facies B, along
608 with the continuation of laminae couplets observed in cores V1 and V2 over the last
609 2 ka, suggests that glaciers reduced in extent at the start of the Holocene but did
610 not disappear completely. It is possible during this transition from Facies A to B,
611 glaciers retreated above Lanezi Lake resulting in more sediment filtering and thus
612 a reduction in sediment delivery and the beginning of seasonally derived laminae
613 couplet formation within Cariboo Lake.

614 Prior to the Neoglacial, sediment accumulation rates are generally lower across
615 western Canada due to reduced glacier extent and warm temperatures (Steinman
616 et al., 2019; Menounos et al., 2004; Koch et al., 2007; Osborn et al., 2007; Luckman,
617 1988, 1993). Therefore, the estimated basal ages of Facies A and B, determined
618 from from sedimentation accumulation rates over the last 2 ka from the long cores
619 presented here, may be much older if the actual sedimentation rates were used. The
620 timing of the transition between these two facies is similar to the onset of deglaciation
621 and start of the Holocene sediment package within Mud Lake, BC (Hodder et al.,
622 2006) around 9.6 ka BP, at Moose Lake, BC (Desloges, 1999) around 10.3 ka BP, at
623 Quesnel Lake, BC (Gilbert and Desloges, 2012) around 8.6 ka BP, and at the Upper
624 Bow River, AB (Leonard and Reasoner, 1999) around 11.7 ka BP. Warming in the early
625 Holocene, around 9.10-6.70 ka BP in the Canadian Rockies, specifically, (Luckman,
626 1986) and British Columbia, generally, (Clague et al., 1989; Steinman et al., 2019) led
627 to two possible sedimentation regimes. Where glaciers persist in the Canadian Rockies
628 through the warm period resulting in more regular seasonality of sediment inputs and

629 laminae couplet formation (e.g. Mud Lake, Hodder et al., 2006) and where glaciers
630 disappear during the warm period, leading to much lower accumulation and seasonality
631 (e.g. Moose Lake, Desloges, 1999).

632 Records of sub-bottom acoustic records from Cariboo Lake present coarse temporal
633 scale resolution of continuous sedimentat accumulation rates throughout the Holocene.
634 Higher resolution AMS dated sediments from the much thinner sediment package in
635 the west arm of Quesnel Lake, located in the Cariboo Mountains (Figure 1), also
636 showed a very consistent mean rate of sedimentation throughout the entire Holocene
637 (Gilbert and Desloges, 2012). Contrasting somewhat from this pattern are results from
638 Menounos et al. (2004) and Desloges (1999) who note that early to mid-Holocene
639 sediment accumulation rates in the southeastern Canadian Cordillera were lower than
640 the late-Holocene Neoglacial period. However, those shifts come from watersheds with
641 much higher percentages of glacier ice cover (~15-40%) coupled with the probable
642 disappearance of glaciers during the warmer hypsithermal. **Therefore**, any extrapolation
643 of timing to the **entire Holocene** sediment record of Cariboo Lake remains speculative.

644 Sediment inputs to Cariboo Lake are mainly delivered via the Cariboo River delta
645 and thus changes in the whole of the Cariboo Lake watershed **would be expected** to
646 be important. In contrast, inputs of sediment from the small tributary watersheds that
647 boarder Cariboo Lake are controlled by more localized, watershed-specific responses.
648 Although coarser grained sediments from discrete turbidite flows are found proximal to
649 sidewall tributary deltas (Figure 5), they are only transferred to deep lake deposits during
650 episodic events (Figure 9). **After removal of instantaneous turbidites, the long core**
651 **sediment records are thought to be most representative of watershed wide trends**
652 **in river discharge influenced by temperature and precipitation rather than isolated**
653 **events and inputs from nearby tributaries and hillslopes.** The long core (V1 and V2)
654 sediment is composed of nearly 99% silt and clay resulting in laminae couplets that are
655 inferred to have been delivered via suspended sediment from the main Cariboo River.
656 Therefore, trends observed in sediment accumulation at cores V1 and V2 likely best
657 represent waterside-wide climate and glacier activity.

658 While cores V1 and V2 do not produce identical results, it is likely the sediment yield
659 data from these cores are within the range of 7-21% error reported in Evans and Church
660 (2000) for other alpine lakes in British Columbia. The inferred error of cores V1 and
661 V2 is attributed to the spatial heterogeneity of sediment accumulation across the Cariboo
662 Lake, and is likely on the lower end of this error range due to its simple basin morphology.
663 Retrieving more than two good long core sedimentary sequences, could have provided a

better estimate in the error of sediment accumulation, however, the logistical demands of retrieving more cores prevented this.

There is a documented range of late Holocene clastic sediment accumulation rates in glacier-fed lakes from across the Canadian Cordillera. Highest rates of $> 2 \text{ cm/yr}$ are observed in ice-contact to ice-proximal lakes of various sizes (Desloges and Gilbert, 1994; Crookshanks and Gilbert, 2008), to relatively low rates of $< 1 \text{ mm yr}^{-1}$ (Gilbert and Desloges, 2012). The range in accumulation rates has been understood to be a result in the variability of sediment production from glacier processes, the steepness of topography (Ballantyne, 2002), the persistence of ice cover and the degree of basin connectivity enhancing or impeding delivery of sediment down valley (Wohl et al., 2019).

In the Cariboo Lake basin, the combination of upper watershed area, intervening storage, glacier cover and lake size are considered optimal during this period for the relatively consistent formation of clastic varves. The Cariboo River has two main tributaries, the Upper Cariboo River and the Matthew River which are connected to high alpine peaks and glaciers providing a significant source of sediment (see Figure 2). Lanezi, Sandy and Ghost lakes act as sediment traps eliminating the transfer of coarse sediment and limiting the transfer of finer sediment from the glacier sediment production zones. This results in sediment accumulation rates that are on the low-end for the southeastern Cordillera (Hodder et al., 2006). Although connectivity is limited, there are sufficient seasonal contrasts in suspended sediment flux to produce couplets (annual varves) in the main basin of Cariboo Lake over the last two millennia. This is unlike the west arm of Quesnel Lake where sediment rates are 2 to 3 times lower due to significant storage in the much larger upper watershed.

Lake sediment chronologies typically vary in their sensitivity to regional fluctuations in temperature and precipitation, from annual resolution in lakes with higher accumulation rates (e.g. Menounos and Clague, 2008) to centennial-scale in lakes with low accumulation rates (e.g. Desloges, 1999). Figure 13a shows the (inferred) varve thickness chronology reconstructed as standardized departures from cores V1 and V2. There is a significant amount of noise in the record, typical of a filtered sediment transport system (e.g. Jerolmack and Paola, 2010), so a lower resolution 30-year moving average is superimposed on the raw couplet thickness data in Figure 13a. Figure 13b and 13c show the lower-resolution temporal patterns in D_{50} grain size and organic matter content, respectively. These trends are compared against the Moberg et al. (2005) regional climate proxy re-analysis for the northern hemisphere (Figure 13d), Solomina et al. (2016) western Canada peak glacier extent estimates (Figure 13e), and Ljungqvist et al. (2016)

699 hydroclimate anomaly estimates for the northern hemisphere (Figure 13f). Most of these
700 are at resolutions of centennial scale or lower.

701 **For Cariboo Lake, above average varve thickness, grain size, and organic matter**
702 **are observed for both V1 and V2 from 2.0-1.3 ka BP. In the southern Coast**
703 **Mountains of British Columbia (Koch et al., 2007; Osborn et al., 2007; Allen and**
704 **Smith, 2007; Clague et al., 2010) and in the Interior ranges and Rocky Mountains**
705 **(Luckman, 1993, 1995) glaciers were generally more extensive prior to 2.0 ka BP**
706 **than present day. More recently than 2.0 ka BP, there is evidence of the First**
707 **Millennium Advance (FMA) primarily from the Coast Mountains (Reyes et al.,**
708 **2006; Osborn et al., 2007) with more recent evidence emerging from the Interior**
709 **Ranges (Maurer et al., 2012). These results cover a range of advance dates between**
710 **1.80 and 1.30 ka BP. The increase in sediment production and sediment availability**
711 **due to extensive glacier advance and then retreat from the FMA may be reflected**
712 **here by the increase in varve thickness and grain size in the Cariboo Lake record**
713 **(Figure 13). Observations of an increase in clastic sedimentation rates in the Rocky**
714 **Mountains were also observed around 1.8 ka BP in Hector Lake (Leonard, 1997).**
715 **Maurer et al. (2012) show that the Castle Creek Glacier intermittently advanced**
716 **into On-off Lake and over the Cariboo River watershed divide throughout the late-**
717 **Holocene between 2.73-2.35, 1.87-1.72, and 1.53-1.42 ka BP (Figure 13). Additional**
718 **contributions of sediment from the Castle Creek Glacier would help contribute to**
719 **above average varve thickness and grain size observed in Cariboo Lake from 2.0-1.3**
720 **ka BP. However, the above average organic matter observed in Figure 13 is atypical**
721 **during an increase of clastic sediment delivery, but could be explained by some**
722 **contributions from increased soil erosion below treeline during a time of higher**
723 **precipitation rates and subsequent high spring freshet flows.**

724 The coarsening trend of grain size from 750-1000 CE in Cariboo Lake is
725 consistent with evidence of an early Little Ice Age (LIA) glacier advance centering
726 around 1250 CE in the Canadian Rockies (Luckman, 1995; Osborn et al., 2001;
727 Leonard, 1997), in the Cariboo Lake basin around 1040-1160 CE (Maurer et al.,
728 2012), and more broadly across western Canada around 1100 CE (Solomina et al.,
729 2016) (Figure 13, D). This period of increased glacier activity also corresponds
730 with the highest temperature anomaly of the Northern Hemisphere MCA (Moberg
731 et al., 2005) (Figure 13). However, Ljungqvist et al. (2016) estimate precipitation
732 to be above average around this time which could have contributed to an increase
733 in glacier extent if corresponding temperatures were low enough. Steinman et al.

734 (2012) studied two lakes in northern Washington, USA which also support above
735 average precipitation for this region during the MCA. Although temperatures are
736 reported as slightly above average during the MCA (Moberg et al., 2005) for the
737 Northern Hemisphere, the increase in glacier activity during this time may have
738 been a result of increased winter precipitation which may have lowered the ELA of
739 glaciers in the Cariboo Lake basin.

740 The second glacier advance of the LIA, which centers around 1850 CE in the
741 Canadian Rockies (Luckman, 2000; Leonard, 1997) coincides with thicker and
742 coarser varves, and a reduction in organic matter in Cariboo Lake (Figure 13).
743 The change in varve thickness, grain size, and organic matter begins earlier for
744 V1 at around 1750 CE compared to V2 which begins to change around 1825 CE.
745 The discrepancy in the sediment characteristic trends between the two cores is
746 considered small given the uncertainty in couplet counting. Overall, the response
747 of varve thickness, grain size, and organic matter to the second advance of the LIA
748 around 1850 CE exhibits a stronger response compared to earlier phases of the LIA.

749 Temperature anomalies for the Northern Hemisphere reported by Moberg et al.
750 (2005), are also most negative from 1500-1750 CE. The dryer conditions reported
751 by Steinman et al. (2012) from 1600-1900 CE, 500 km south of Cariboo Lake
752 in Castor and Lime Lakes could be attributed to a strong negative temperature
753 anomaly. These records suggest there was a strong influence of the LIA climate on
754 glacier activity in the region compared to the rest of the 2 ka record. Following the
755 LIA, around 2000 CE a dramatic decline in organic matter and increase in grain
756 size is observed suggestive of high magnitude clastic sediment delivery. This could
757 be attributed to the increase of sediment availability as glaciers retreated more
758 rapidly from LIA extents and exposed stores of clastic sediments (Beedle et al.,
759 2015). However, hydraulic mining practices during the Cariboo Gold Rush and
760 deforestation began during the late 1800s and they also may have contributed to
761 this rapid increase. Human disturbance related controls on sediment inputs for the
762 last 100 years or more are known to confound the climate-glacier-sediment output
763 signal (Beedle et al., 2015).

764 Conclusions

765 The moderated-sized Cariboo Lake provides a very good record of deglacial and
766 Holocene sediment inputs for central British Columbia. The steep climatic gradient from

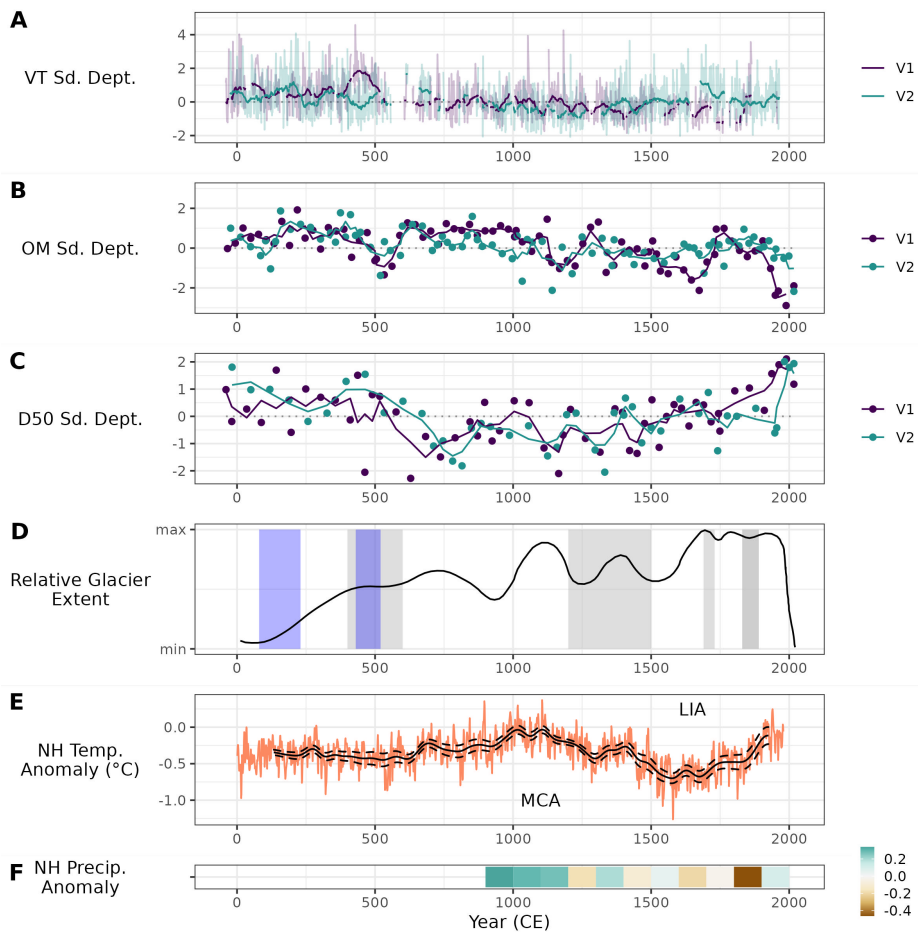


Figure 13. Cariboo Lake sediment characteristics for cores V1 (purple) and V2 (green) and Northern Hemisphere (NH) climate proxies. A, is the standardized departure (Sd. Dept.) from the mean varve thickness (VT) for annual couplets (light colour) and 30-year moving average (dark lines). B, is the standardized departure from the mean percent organic matter (OM) for cores V1 and V2. The coloured dots represent percent OM at 2.5 - 5 cm intervals and the coloured lines are the 3 sample (75 year) moving average. C, is the standardized departure from the mean D 50 grain size, the coloured dots represent D 50 grain size at 5 - 10 cm intervals and the coloured lines are the 3 sample (125 year) moving average. D, Moberg et al. (2005) Nothern Hemisphere annual temperature anomaly from the 1961-1990 mean, the orange line is the full reconstruction from high and low frequency proxies, and the black line is the low frequency proxy component with upper and lower uncertainty marked by dashed blue lines. MCA is the Medieval Climatic Anomaly and LIA is the Little Ice Age. E, Solomina et al. (2016) reconstructed relative glacier extent in western North America (black line), expansion of the Castle Creek glacier (blue bars, Maurer et al., 2012), and periods of peak glacier extent in western Canada (gray bars, Solomina et al., 2016). F, Ljungqvist et al. (2016) Nothern Hemisphere hydroclimate variability, expressed as standardized unitless anomalies ranging from -2 to 2, relative to the centennial mean and standard deviation over the eleventh-nineteenth centuries (see methods in Ljungqvist et al. 2016).

767 the wetter, glacier covered, headwaters to the semi-arid, lower elevation zones of the
768 lake, result in sediment input via the main Cariboo Lake delta that is predominately
769 derived from the glacier production zone. This conclusion is supported by the down-lake
770 trends observed in grain-size and organic matter content. The smaller alluvial-fan deltas
771 from side tributaries appear to be paraglacial relic features, similar to those described
772 in Church and Ryder (1972), and likely formed during deglaciation and the earliest
773 Holocene as no evidence of significant inputs during the Holocene were found in this
774 study.

- 775 1. Sub-bottom acoustic records provide a coarse temporal resolution chronology of
776 early and mid-Holocene sediment accumulation. **The transition from massive to
777 acoustically well-layered sediments is estimated to have occurred around 10.5
778 to 9 ka BP. There is uncertainty with the timing of this transition as sediment
779 accumulation rates have been extrapolated from the 2 ka old sediment cores.**
780 Still, the 10.5 to 9 ka BP transition is similar to other glacier, lake and climate
781 records across British Columbia and Alberta suggesting fairly consistent and rapid
782 withdrawal of valley-bottom glacier ice into higher elevation zones.
- 783 2. **There were limitations in the ability to retrieve sufficiently long cores (> 10-
784 15 m), that would provide a high resolution record of sediment inputs to
785 Cariboo Lake over the entire Holocene.** If trends observed in other southern
786 Canadian Cordilleran lakes prevail, the early and mid-Holocene input of sediment
787 during the hyspothermal would have been significantly reduced resulting in a
788 Holocene sediment package within the 10-15 m range. Acoustic Facies B most
789 likely represents this unit.
- 790 3. Sedimentary structures in the long cores indicated sediment delivery, over the
791 late Holocene to present, is dominated by similar fractions of silt (spring freshet)
792 and clay (winter settling) resulting in the formation of rhythmically laminated
793 couplets that are mainly varves. **The fraction of fine clastic sediments observed
794 in the Cariboo Lake cores is high compared to other lakes in the Canadian
795 Cordillera which typically have a larger fraction of coarse sediment from
796 more frequent fall or spring high flows.** While there is relatively close agreement
797 between sediment chronology from laminae counting and the two AMS dates,
798 it is not possible to develop a chronology that provides a precisely dated high-
799 resolution sediment yield record over the last 2 ka. However, the observed mean
800 accumulation rate (**1.6 mm yr⁻¹**), the variance in accumulation rates and the low-
801 frequency trends are important indicators of late Holocene environmental change.

-
- 802 **4. Periods of peak glacier extent, such as during the First Millennial Advance**
803 (\sim 200 to 700 CE) and Little Ice Age (\sim 1600 to 1900 CE) are best correlated with
804 grain size in Cariboo Lake. The trends in varve thickness were not as strong
805 but still help confirm trends observed in grain size. Organic matter content is
806 the least correlated with the other sediment metrics and may be more sensitive
807 to vegetation changes in the basin. We conclude that sediment accumulation in
808 Cariboo Lake was more sensitive to glacier activity and sediment production
809 during the LIA compared to earlier advances.
- 810 5. The greatest deviation in varve thickness, grain size, and organic matter above
811 normal occurs after 1860 CE and may be related to climate warming following the
812 LIA. However, there are complications in this watershed via large-scale mining
813 proximal to the lake and some upper watershed deforestation. These land-use
814 and land-cover changes may have also been contributing factors to an increase
815 in sediment delivery to the lake.
- 816 6. **Upstream filtering and storage of glacier eroded sediment may reduce the**
817 **strength of the climate-sediment signal for Cariboo Lake.** However, there
818 is ample evidence that the sediment record spanning the last 2000 years
819 gives better temporal resolution of watershed dynamics compared to other
820 available records in the Interior Ranges of British Columbia. While the results
821 presented here broadly agree with the primary glacier advances over the past
822 2000 years, further study of the laminated Cariboo Lake sediment record
823 is required to better determine the exact timing and importance (i.e. signal
824 strength) of sediment inputs related to shifts of climate and glacier activity
825 across of the south eastern Canadian Cordillera.

826 Acknowledgements

827 We thank Michael Allchin, Laszlo Enyedy, and Caitlin Langford at the Quesnel River
828 Research Centre for assistance in field. Brian Menounos kindly provided access to vibra-
829 coring equipment. Mike Gorton, George Kretschmann, Anna Soleski and Selina Amaral
830 provided assistance with lab analysis of sediment samples. Funding was provided by the
831 University of Toronto.

References

- Allen SM and Smith DJ (2007) Late Holocene glacial activity of Bridge Glacier, British Columbia Coast Mountains. *Canadian Journal of Earth Sciences* 44(12): 1753–1773. DOI:10.1139/E07-059.
- Ballantyne CK (2002) Paraglacial geomorphology. *Quaternary science reviews* 21(18): 1935–2017.
- Beedle MJ, Menounos BP and Wheate R (2015) Glacier change in the Cariboo Mountains, British Columbia, Canada (1952–2005). *Cryosphere* 9(1): 65–80. DOI:10.5194/tc-9-65-2015.
- Bolch Ts and Bolch Ta (2008) GLIMS Glacier Database. DOI:10.7265/N5V98602.
- Brown KJ, Fitton RJ, Schoups G, Allen GB, Wahl KA and Hebda RJ (2006) Holocene precipitation in the coastal temperate rainforest complex of southern British Columbia, Canada. *Quaternary Science Reviews* 25(21–22): 2762–2779. DOI:10.1016/j.quascirev.2006.02.020.
- Church M and Ryder JM (1972) Paraglacial Sedimentation: A Consideration of Fluvial Processes Conditioned by Glaciation. *GSA Bulletin* 83(10): 3059–3072. DOI:10.1130/0016-7606(1972)83[3059:PSACOF]2.0.CO;2. URL [https://doi.org/10.1130/0016-7606\(1972\)83\[3059:PSACOF\]2.0.CO;2](https://doi.org/10.1130/0016-7606(1972)83[3059:PSACOF]2.0.CO;2).
- Clague JJ, Koch J and Geertsema M (2010) Expansion of outlet glaciers of the Juneau Icefield in northwest British Columbia during the past two millennia. *The Holocene* 20(3): 447–461. DOI:10.1177/0959683609353433. URL <https://doi.org/10.1177/0959683609353433>.
- Clague JJ, Mathews W, Ryder J, Hughes O, Rutter NW, Jackson L, Matthews J and MacDonald G (1989) Quaternary geology of the Canadian Cordillera. In: *Quaternary geology of Canada and Greenland*. North America: Geological Society of America, pp. 15–96. DOI:10.1130/dnag-gna-k1.15. URL <https://pubs.geoscienceworld.org/books/book/853/chapter/4856715/>.
- Cockburn JM and Lamoureux SF (2008) Inflow and lake controls on short-term mass accumulation and sedimentary particle size in a High Arctic lake: Implications for interpreting varved lacustrine sedimentary records. *Journal of Paleolimnology* 40(3): 923–942. DOI:10.1007/s10933-008-9207-5.
- Crookshanks S and Gilbert R (2008) Continuous, diurnally fluctuating turbidity currents in Kluane Lake, Yukon Territory. *Canadian journal of earth sciences* 45(10): 1123–1138.
- Desloges JR (1999) Geomorphic and climatic interpretations of abrupt changes in glaciolacustrine deposition at Moose Lake, British Columbia, Canada. *Gff* 121(3): 202–207. DOI:10.1080/1103589901213202.

- 866 Desloges JR and Gilbert R (1994) Sediment source and hydroclimatic inferences from glacial lake
867 sediments: the postglacial sedimentary record of Lillooet Lake, British Columbia. *Journal
868 of Hydrology* 159(1-4): 375–393. DOI:10.1016/0022-1694(94)90268-2. URL <https://www.sciencedirect.com/science/article/pii/0022169494902682>.
- 870 Dirsztowsky RW and Desloges JR (1997) Glaciolacustrine sediments and neoglacial history of the
871 Chephren lake basin, Banff National Park, Alberta. *Geographie Physique Et Quaternaire*
872 51(1): 41–53. DOI:10.7202/004804ar.
- 873 Filippelli GM, Souch C, Menounos B, Slater-Atwater S, Timothy Jull AJ and Slaymaker O
874 (2006) Alpine lake sediment records of the impact of glaciation and climate change on the
875 biogeochemical cycling of soil nutrients. *Quaternary research* 66(1): 158–166.
- 876 Gardner JS and Jones NK (1985) Evidence for a Neoglacial advance of the Boundary Glacier,
877 Banff National Park, Alberta. *Canadian Journal of Earth Sciences* 22(11): 1753–1755. DOI:
878 10.1139/e85-185. URL <https://doi.org/10.1139/e85-185>.
- 879 Gilbert R and Desloges JR (2012) Late glacial and Holocene sedimentary environments of Quesnel
880 Lake, British Columbia. *Geomorphology* 179: 186–196. DOI:10.1016/j.geomorph.2012.08.
881 010. URL <http://dx.doi.org/10.1016/j.geomorph.2012.08.010>.
- 882 Gilbert R, Desloges JR and Clague J (1997) The glaciolacustrine sedimentary environment of
883 Bowser Lake in the northern Coast Mountains of British Columbia, Canada. *Journal of
884 Paleolimnology* 17(3): 333–348. DOI:10.1023/A:1007900411724. URL <http://link.springer.com/10.1023/A:1007900411724>.
- 886 Gray AB, Pasternack GB and Watson EB (2010) Hydrogen peroxide treatment effects on the
887 particle size distribution of alluvial and marsh sediments. *The Holocene* 20(2): 293–301.
888 DOI:10.1177/0959683609350390. URL <http://journals.sagepub.com/doi/10.1177/0959683609350390>.
- 890 Hallett DU, Hills LV and Clague JJ (1997) New accelerator mass spectrometry radiocarbon ages for
891 the Mazama tephra layer from Kootenay National Park, British Columbia, Canada. *Canadian
892 Journal of Earth Sciences* 34(9): 1202–1209. DOI:10.1139/e17-096.
- 893 Harvey JE, Smith DJ, Laxton S, Desloges J and Allen S (2012) Mid-Holocene glacier expansion
894 between 7500 and 4000 cal. yr BP in the British Columbia Coast Mountains, Canada. *Holocene*
895 22(9): 975–985. DOI:10.1177/0959683612437868.
- 896 Haslett J and Parnell A (2008) A simple monotone process with application to radiocarbon-dated
897 depth chronologies. *Applied statistics* 57(4): 399–418.
- 898 Heideman M, Menounos B and Clague JJ (2018) A multi-century estimate of suspended sediment
899 yield from Lillooet Lake, southern Coast Mountains, Canada. *Canadian journal of earth*

- 900 *sciences* 55(1): 18–32.
- 901 Heideman M, Menounos BP and Clague J (2015) An 825-year long varve record from Lillooet
902 Lake, British Columbia, and its potential as a flood proxy. *Quaternary Science Reviews* 126:
903 158–174. DOI:10.1016/j.quascirev.2015.08.017. URL <http://dx.doi.org/10.1016/j.quascirev.2015.08.017>.
- 904 Hodder KR, Desloges JR and Gilbert R (2006) Pattern and timing of sediment infill at glacier-fed Mud Lake: Implications for lateglacial and Holocene environments in the Monashee Mountain region of British Columbia, Canada. *Holocene* 16(5): 705–716. DOI:10.1191/0959683606hl965rp.
- 905 Hodder KR, Gilbert R and Desloges JR (2007) Glaciolacustrine varved sediment as an alpine hydroclimatic proxy. *Journal of Paleolimnology* 38(3): 365–394. DOI:10.1007/s10933-006-9083-9.
- 906 Huber M and Knutti R (2012) Anthropogenic and natural warming inferred from changes in Earth's energy balance. *Nature geoscience* 5(1): 31–36.
- 907 Jerolmack DJ and Paola C (2010) Shredding of environmental signals by sediment transport. *Geophysical research letters* 37(19): n/a.
- 908 Koch J, Osborn GD and Clague JJ (2007) Pre-'Little Ice Age' glacier fluctuations in Garibaldi Provincial Park, Coast Mountains, British Columbia, Canada. *Holocene* 17(8): 1069–1078. DOI:10.1177/0959683607082546.
- 909 Leonard EM (1986) Use of lacustrine sedimentary sequences as indicators of Holocene glacial history, Banff National Park, Alberta, Canada. *Quaternary Research* 26(2): 218–231. DOI: 10.1016/0033-5894(86)90106-7.
- 910 Leonard EM (1997) The relationship between glacial activity and sediment production: Evidence from a 4450-year varve record of neoglacial sedimentation in Hector Lake, Alberta, Canada. *Journal of Paleolimnology* 17(3): 319–330.
- 911 Leonard EM and Reasoner MA (1999) A continuous holocene glacial record inferred from proglacial lake sediments in Banff National Park, Alberta, Canada. *Quaternary Research* 51(1): 1–13. DOI:10.1006/qres.1998.2009. URL <https://www.sciencedirect.com/science/article/pii/S0033589498920099>.
- 912 Ljungqvist FC, Krusic PJ, Sundqvist HS, Zorita E, Brattstrom G and Frank D (2016) Northern hemisphere hydroclimate variability over the past twelve centuries. *Nature* 532: 94+. URL <https://link.gale.com/apps/doc/A449108229/EAIM?u=usaskmain&sid=bookmark-EAIM&xid=1dfbd232>.

- 933 Lowe DJ, Green JD, Northcote TG and Hall KJ (1997) Holocene Fluctuations of a Meromictic
934 Lake in Southern British Columbia. *Quaternary research* 48(1): 100–113.
- 935 Luckman BH (1986) Reconstruction of Little Ice Age Events in the Canadian Rocky Mountains.
936 *Géographie physique et quaternaire* 40(1): 17–28.
- 937 Luckman BH (1988) 8000 year old wood from the Athabasca Glacier, Alberta. *Canadian*
938 *Journal of Earth Sciences* 25(1): 148–151. DOI:10.1139/e88-015. URL <http://www.nrcresearchpress.com/doi/10.1139/e88-015>.
- 939 Luckman BH (1993) Glacier fluctuation and tree-ring records for the last millennium in
940 the Canadian Rockies. *Quaternary Science Reviews* 12(6): 441–450. DOI:10.1016/S0277-3791(05)80008-3.
- 941 Luckman BH (1995) Calendar-dated, early ‘Little Ice Age’ glacier advance at Robson
942 Glacier, British Columbia, Canada. *The Holocene* 5(2): 149–159. DOI:10.1177/
943 095968369500500203.
- 944 Luckman BH (2000) The Little Ice Age in the Canadian Rockies. *Geomorphology*
945 32(3-4): 357–384. DOI:10.1016/S0169-555X(99)00104-X. URL <http://linkinghub.elsevier.com/retrieve/pii/S0169555X9900104X%5Cnfile:///Users/whobbs/Documents/PDFs/Papers2/Luckman/2000/Geomorphology2000Luckman.pdf%5Cnpapers2://publication/uuid/7AE71933-5443-41E0-B7B7-88A14B3C077A>.
- 946 Luckman BH and Kavanagh T (2000) Impact of climate fluctuations on mountain environments
947 in the Canadian Rockies. *Ambio* 29(7): 371–380. DOI:10.1639/0044-7447(2000)029[0371:IOCFOM]2.0.CO;2.
- 948 Luckman BH, Kavanagh TA, Craig I and St George RS (1999) Earliest photograph of Athabasca
949 and Dome Glaciers, Alberta. *Géographie physique et Quaternaire* 53(3): 401. DOI:
950 10.7202/004844ar. URL <http://id.erudit.org/iderudit/004844ar>.
- 951 Masson-Delmotte V, Schulz M, Abe-Ouchi A, Beer J, Ganopolski J, González Rouco JF, Jansen
952 E, Lambeck K, Luterbacher J, Naish T, Osborn T, Otto-Bliesner B, Quinn T, Ramesh R, Rojas
953 M, Shao X and Timmermann A (2013) *Information from paleoclimate archives*. Cambridge,
954 United Kingdom and New York, NY, USA.: Cambridge University Press, pp. 383–464. DOI:
955 10.1017/CBO9781107415324.013.
- 956 Maurer MK, Menounos BP, Luckman BH, Osborn GD, Clague J, Beedle MJ, Smith R and
957 Atkinson N (2012) Late Holocene glacier expansion in the Cariboo and northern Rocky
958 Mountains, British Columbia, Canada. *Quaternary Science Reviews* 51: 71–80. DOI:10.
959 1016/j.quascirev.2012.07.023. URL <https://www.sciencedirect.com/science>

- 967 [article/pii/S0277379112002909http://resolver.scholarsportal.info/resolve/02773791/v51inone_c/71_lhgeitnrbcc](http://resolver.scholarsportal.info/resolve/02773791/v51inone_c/71_lhgeitnrbcc).
- 968
- 969 Menounos BP and Clague JJ (2008) Reconstructing hydro-climatic events and glacier fluctuations
970 over the past millennium from annually laminated sediments of Cheakamus Lake, southern
971 Coast Mountains, British Columbia, Canada. *Quaternary Science Reviews* 27(7-8): 701–713.
972 DOI:10.1016/j.quascirev.2008.01.007.
- 973 Menounos BP, Koch J, Osborn GD, Clague J and Mazzucchi D (2004) Early Holocene glacier
974 advance, southern Coast Mountains, British Columbia, Canada. *Quaternary Science Reviews*
975 23(14-15): 1543–1550. DOI:10.1016/j.quascirev.2003.12.023. URL <https://www.sciencedirect.com/science/article/pii/S027737910400023X>.
- 976 Menounos BP, Osborn GD, Clague J and Luckman BH (2009) Latest Pleistocene and Holocene
977 glacier fluctuations in western Canada. *Quaternary Science Reviews* 28(21-22): 2049–2074.
978 DOI:10.1016/j.quascirev.2008.10.018.
- 979 Menounos BP, Schiefer E and Slaymaker O (2006) Nested temporal suspended sediment yields,
980 Green Lake Basin, British Columbia, Canada. *Geomorphology* 79(1-2): 114–129. DOI:
981 10.1016/j.geomorph.2005.09.020.
- 982 Moberg A, Sonechkin DM, Holmgren K, Datsenko MH and Karlén W (2005) Highly variable
983 Northern Hemisphere temperatures reconstructed from low- and high-resolution proxy data.
984 *Nature* 433(7026): 613–617. DOI:10.1038/nature03265.
- 985 Nelson MC, Ingram SE, Dugmore AJ, Streeter R, Peebles MA, McGovern TH, Hegmon M,
986 Arneborg J, Kintigh KW, Brewington S, Spielmann KA, Simpson IA, Strawhacker C, Comeau
987 LEL, Torvinen A, Madsen CK, Hambrecht G and Smiarowski K (2016) Climate challenges,
988 vulnerabilities, and food security. *Proceedings of the National Academy of Sciences* 113(2):
989 298–303. DOI:10.1073/pnas.1506494113. URL <https://www.pnas.org/doi/abs/10.1073/pnas.1506494113>.
- 990 Neukom R, Barboza LA, Erb MP, Shi F, Emile-Geay J, Evans MN, Franke JJ, Kaufman DS,
991 Lücke L, Rehfeld K, Schurer A, Zhu F, Brönnimann S, Hakim GJ, Henley BJ, Ljungqvist
992 FC, McKay N, Valler V, von Gunten L, Lucke L, Rehfeld K, Schurer A, Zhu F, Brönnimann
993 S, Hakim GJ, Henley BJ, Ljungqvist FC, McKay N, Valler V and von Gunten L (2019)
994 Consistent multidecadal variability in global temperature reconstructions and simulations over
995 the Common Era. *Nature geoscience* 12(8): 643–649. DOI:10.1038/s41561-019-0400-0.
- 996 Osborn GD, Menounos BP, Koch J, Clague J and Vallis V (2007) Multi-proxy record of Holocene
997 glacial history of the Spearhead and Fitzsimmons ranges, southern Coast Mountains, British
998 Columbia. *Quaternary Science Reviews* 26(3-4): 479–493. DOI:10.1016/j.quascirev.2006.09.

- 1001 003.
- 1002 Osborn GD, Robinson BJ and Luckman BH (2001) Holocene and latest Pleistocene fluctuations of
1003 Stutfield Glacier, Canadian Rockies. *Canadian Journal of Earth Sciences* 38(8): 1141–1155.
1004 DOI:10.1139/e01-012.
- 1005 Parnell AC, Buck CE and Doan TK (2011) A review of statistical chronology models for high-
1006 resolution, proxy-based Holocene palaeoenvironmental reconstruction. *Quaternary science*
1007 reviews 30(21): 2948–2960.
- 1008 Parnell AC, Haslett J, Allen JRM, Buck CE and Huntley B (2008) A flexible approach to
1009 assessing synchronicity of past events using Bayesian reconstructions of sedimentation history.
1010 *Quaternary science reviews* 27(19): 1872–1885.
- 1011 Reimer PJ, Bard E, Bayliss A, Beck JW, Blackwell PG, Bronk Ramsey C, Buck CE, Cheng H,
1012 Edwards RL, Frieich M, Grootes PM, Guilderson TP, Haflidason H, Hajdas I, Hatté C, Heaton
1013 TJ, Hoffmann DL, Hogg AG, Hughen KA, Kaiser KF, Kromer B, Manning SW, Niu M,
1014 Reimer RW, Richards DA, Scott EM, Southon JR, Staff RA, Turney CSM and van der Plicht
1015 J (2013) IntCal13 and Marine13 Radiocarbon Age Calibration Curves 0–50,000 Years cal BP.
1016 *Radiocarbon* 55(4): 1869–1887.
- 1017 Reyes ADV, Wiles GC, Smith DJ, Barclay DJ, Allen Scott Jackson Sonya Larocque Sarah Laxton
1018 Dave Lewis S, Calkin PE and Clague J (2006) Expansion of alpine glaciers in Pacific North
1019 America in the first millennium A. *Geology* 34(3). DOI:10.1130/G21902.1. URL [https://www.sfu.ca/\\$\sim\\$gqrc/papers/1stmillenniumADadvance.pdf](https://www.sfu.ca/\simgqrc/papers/1stmillenniumADadvance.pdf).
- 1020 Ryder JM and Thomson B (1986) Neoglaciation in the southern Coast Mountains of
1021 British Columbia: chronology prior to the late Neoglacial maximum. *Canadian Journal*
1022 of *Earth Sciences* 23(3): 273–287. DOI:10.1139/e86-031. URL <http://www.nrcresearchpress.com/doi/10.1139/e86-031>.
- 1023 Sabatier P, Moernaut J, Bertrand S, Daele MV, Kremer K, Chaumillon E, Arnaud F, Van Daele
1024 M, Kremer K, Chaumillon E and Arnaud F (2022) A Review of Event Deposits in Lake
1025 Sediments. *Quaternary* 5(3): 34. DOI:10.3390/quat5030034.
- 1026 Schneider CA, Rasband WS and Eliceiri KW (2012) NIH Image to ImageJ: 25 years of image
1027 analysis. *Nature Methods* 9(7): 671–675. DOI:10.1038/nmeth.2089. URL <https://doi.org/10.1038/nmeth.2089>.
- 1028 Smith JG (2003) Aspects of the loss-on-ignition (loi) technique in the context of clay-rich,
1029 glaciolacustrine sediments. *Geografiska Annaler: Series A, Physical Geography* 85(1): 91–
1030 97. DOI:10.1111/1468-0459.00191. URL <https://www.tandfonline.com/doi/full/10.1111/1468-0459.00191>.
- 1031
- 1032
- 1033
- 1034

- 1035 Solomina ON, Bradley RS, Jomelli V, Geirsdottir A, Kaufman DS, Koch J, McKay NP, Masiokas
1036 M, Miller G, Nesje A, Nicolussi K, Owen LA, Putnam AE, Wanner H, Wiles G and Yang
1037 B (2016) Glacier fluctuations during the past 2000 years. *Quaternary Science Reviews* 149:
1038 61–90. DOI:10.1016/j.quascirev.2016.04.008.
- 1039 Steinman BA, Abbott MB, Mann ME, Stansell ND and Finney BP (2012) 1,500 year quantitative
1040 reconstruction of winter precipitation in the Pacific Northwest. *Proceedings of the National
1041 Academy of Sciences* 109(29): 11619–11623. DOI:10.1073/pnas.1201083109. URL <http://www.pnas.org/cgi/doi/10.1073/pnas.1201083109>.
- 1042 Steinman BA, Nelson DB, Abbott MB, Stansell ND, Finkenbinder MS and Finney BP (2019)
1043 Lake sediment records of Holocene hydroclimate and impacts of the Mount Mazama eruption,
1044 north-central Washington, USA. *Quaternary Science Reviews* 204: 17–36. DOI:10.1016/
1045 j.quascirev.2018.09.018. URL [https://doi.org/10.1016/j.quascirev.2018.
1046 09.018](https://doi.org/10.1016/j.quascirev.2018.09.018).
- 1047 Turney CSM, McGregor HV, Francus P, Abram N, Evans MN, Goosse H, Von Gunten L, Kaufman
1048 D, Linderholm H, Loutre MF and Neukom R (2019) Introduction to the special issue "climate
1049 of the past 2000 years: Regional and trans-regional syntheses". *Climate of the past* 15(2):
1050 611–615.
- 1051 Westgate JA (1977) Identification and Significance of Late Holocene Tephra From Otter Creek,
1052 Southern British Columbia, and Localities in West-Central Alberta. *Can J Earth Sci* 14(11):
1053 2593–2600. DOI:10.1139/e77-224.
- 1054 Wohl E, Brierley G, Cadol D, Coulthard TJ, Covino T, Fryirs KA, Grant G, Hilton RG, Lane SN,
1055 Magilligan FJ, Meitzen KM, Passalacqua P, Poeppel RE, Rathburn SL and Sklar LS (2019)
1056 Connectivity as an emergent property of geomorphic systems. *Earth Surface Processes and
1057 Landforms* 44(1): 4–26. DOI:10.1002/esp.4434.
- 1058 Wood C and Smith DJ (2004) Dendroglaciological Evidence For A Neoglacial Advance Of the
1059 Saskatchewan Glacier, Banff National Park, Canadian Rocky Mountains. *Tree-Ring Research*
1060 60(1): 59–65. DOI:10.3959/1536-1098-60.1.59.
- 1061 Zdanowicz CM, Zielinski GA and Germani MS (1999) Mount Mazama eruption: Calendrical
1062 age verified and atmospheric impact assessed. *Geology* 27(7): 621–624. DOI:10.1130/
1063 0091-7613(1999)027<0621:MMECAV>2.3.CO;2.
- 1064 Zolitschka B (1991) Absolute dating of late quaternary lacustrine sediments by high resolution
1065 varve chronology. *Hydrobiologia* 214(1): 59–61.
- 1066 Zolitschka B, Francus P, Ojala AE and Schimmelmann A (2015) Varves in lake sediments - a
1067 review. *Quaternary Science Reviews* 117: 1–41. DOI:10.1016/j.quascirev.2015.03.019. URL

1069 <http://dx.doi.org/10.1016/j.quascirev.2015.03.019>.